Inorganic Chemistry

Article

pubs.acs.org/IC

# Reactivity Studies on [Cp′FeI]$_2$: Monomeric Amido, Phenoxo, and Alkyl Complexes

Marc D. Walter*[,†] and Peter S. White[‡]

[†]Institut für Anorganische und Analytische Chemie, Technische Universität Braunschweig, Hagenring 30, 38106 Braunschweig, Germany

[‡]Department of Chemistry, University of North Carolina at Chapel Hill, Chapel Hill, North Carolina 27599-3290, United States

Supporting Information

**ABSTRACT:** A series of monomeric mono(cyclopentadienyl) iron amido, phenoxo, and alkyl complexes were synthesized, and their structure and reactivity are presented. The iron(II) centers in these 14VE one-legged piano stool complexes are high spin ($S$ = 2) in solid state and solution independent of solvent. The silylamide compound [Cp′FeN(SiMe$_3$)$_2$] (**2a**, Cp′ = 1,2,4-(Me$_3$C)$_3$C$_5$H$_2$) is an excellent starting material for the reaction with more acidic substrates such as phenols. Sterically encumbered phenols 2,6-(Me$_3$C)$_2$(4-R)C$_6$H$_2$OH (R = H, Me, and *t*Bu) were investigated. In all cases monomeric iron phenoxo half-sandwich complexes [Cp′FeOR′] (**4-R**) are initially formed. Rearrangement of **4-R** to the diamagnetic oxocyclohexadienyl complex [Cp′Fe($\eta^5$-O=C$_6$H$_2$R′$_2$R″)] (**5-R**) is observed for 2,6-(Me$_3$C)$_2$(4-R)C$_6$H$_2$OH (R = H and Me) and the Gibbs free enthalpy of activation ($\Delta G^{\ddagger}$) was determined. In contrast this rearrangement is inhibited when the 4-position is blocked by a *t*Bu group. Removing the steric bulk from the 2,6-positions leads to the formation of a $\mu$-phenoxo dimer, [Cp′Fe($\mu$-OC$_6$H$_3$*t*Bu$_2$-3,5)]$_2$ (**5**). Density functional theory (DFT) was used to further elucidate the structure−reactivity relationship in these molecules. The one-legged piano stool anilido complex [Cp′Fe(NHC$_6$H$_2$*t*Bu$_3$-2,4,6)] (**7**) is not accessible via acid−base reaction between **2a** and H$_2$NC$_6$H$_2$*t*Bu$_3$-2,4,6, but can be prepared by conventional salt metathesis reaction from [Cp′FeI]$_2$ and [Li(NHC$_6$H$_2$*t*Bu$_3$-2,4,6)(OEt$_2$)]$_2$. In contrast, reaction of **2a** with Ph$_2$NH yields the bimetallic [Cp′Fe(*N*,*C*-$\kappa^1$,$\eta^5$-C$_6$H$_5$NPh)Fe(*N*-$\kappa^1$-NPh$_2$)Cp′] (**8**) which combines two iron centers in the same oxidation state (+2), but different spin-states ($S$ = 0 and $S$ = 2) which is reflected in very different Cp(cent)−Fe distances of 1.68 and 2.04 Å, respectively. A monomeric iron alkyl half-sandwich complex [Cp′FeCH(SiMe$_3$)$_2$] (**9**) was prepared that exhibits no reactivity toward H$_2$, C$_2$H$_4$ or N$_2$O. This behavior might be rationalized by a spin-state induced reaction barrier. However, **9** reacts in the presence of CO to the iron acyl-complex [Cp′Fe(CO)$_2$(C(O)CH(SiMe$_3$)$_2$)] (**10**) and with a CO/H$_2$ mixture [Cp′Fe(CO)$_2$]$_2$ (**11**) and CH$_2$(SiMe$_3$)$_2$ are formed.

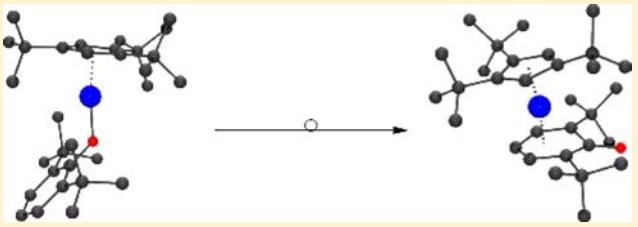

## INTRODUCTION

Low-coordinate iron complexes have been explored as possible models systems for the active sites in metalloenzymes, and many groups have made important contributions in this area.[1−4] Sterically demanding ligands are a common motive in these investigations since they allow highly unusual molecules to be synthesized and their chemistry to be explored.[3,5−15] Ligands of choice have been based on scorpionates or Schiff-base ligands because of their excellent donor capabilities and highly modular ligand architectures which allow for easy variations of the steric and electronic properties.

However, in contrast to the rich and versatile ruthenium half-sandwich chemistry,[16−24] low-coordinate, open-shell mono(cyclopentadienyl) iron complexes have not been explored extensively. The competitive formation of thermodynamically favored ferrocene, [(C$_5$H$_5$)$_2$Fe], required the use of sterically demanding alkylcyclopentadienyl ligands for the isolation and stabilization of low-coordinate high spin mono(cyclopentadienyl) iron(II) complexes. The kinetic stability of these complexes stems from the effective blocking of the dismutation pathway. Sitzmann and co-workers reported the synthesis of [($^n$Cp)FeBr]$_2$ ($^5$Cp = C$_5$(CHMe$_2$)$_5$, $^4$Cp = C$_5$H(CHMe$_2$)$_4$ and Cp′ = 1,2,4-(Me$_3$C)$_3$C$_5$H$_2$) without additional donor ligands several years ago.[25,26] These complexes can be isolated as stable compounds, and they react with substituted phenolates to yield monomeric and dimeric complexes depending on the steric bulk of the phenolate ligand.[26] Aryl ligands connected to the Cp′Fe-fragment have been reported to undergo $\sigma/\pi$-rearrangements,[27−29] whereas the related [$^5$CpFe(C$_5$H$_3$*i*Pr$_2$-2,6)] complex behaves as a single-molecule magnet.[30] [(C$_5$Me$_5$)FeN(SiMe$_3$)$_2$] belongs to the same class of iron one-legged piano stools[31] and exhibits promising synthetic potential.[32,33] In general, silylamide metal complexes can readily deprotonate more acidic substrates, and they have been used to generate homo- and heteroleptic metal complexes.[34−44]

**Received:** August 13, 2012
**Published:** October 15, 2012

 © 2012 American Chemical Society  dx.doi.org/10.1021/ic301770f | *Inorg. Chem.* 2012, 51, 11860−11872

**Scheme 1**

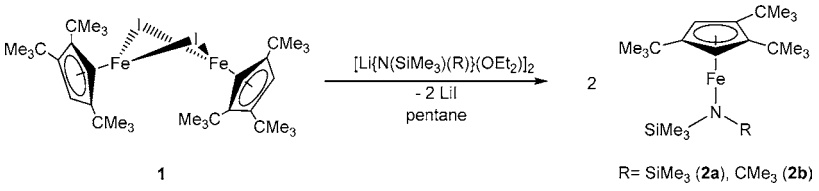


On the basis of this precedence, we have recently initiated an active research program focusing on the reactivity of $[Cp'FeI]_2$ (**1**) and its potential in the synthesis of synthetically attractive target molecules. During these investigations we have shown that **1** is a good synthon for $[Cp'Fe]^+$ transfer to Ir pincer complexes,[45] and for the synthesis of iron polyhydrides, $[Cp'_2Fe_2H_3]$ and $[Cp'FeH_2]_2$. In addition, $[Cp'FeH_2]_2$ acts as Fe(I) synthon which efficiently activate white phosphorus ($P_4$).[46] Furthermore, **1** can be used for the synthesis of $[Cp'Fe\{N(SiMe_3)_2\}]$ (**2a**) which reacts with water in an acid–base reaction to yield the trimeric iron hydroxo complex, $[Cp'Fe(\mu\text{-}OH)]_3$.[47] In this contribution, we focus on the synthesis of additional one-legged piano stools of the type "Cp′FeX", where X = phenolato, anilido, and alkyl groups, and discuss their structure and reactivity.

## RESULTS AND DISCUSSION

**Iron Amides.** Complex **1** is an excellent starting material for monomeric 14 valence electron (VE) iron amide complexes such as $[Cp'Fe\{N(SiMe_3)(R)\}]$ (R = $SiMe_3$ (**2a**),[47] $CMe_3$ (**2b**)) which are readily prepared by salt metathesis between **1** and $[Li\{N(SiMe_3)(R)\}(OEt_2)]_2$ in aliphatic solvents such as pentane (Scheme 1). They are very soluble in all common organic solvents, but can be obtained as yellow crystals by sublimation or crystallization from concentrated $(Me_3Si)_2O$ solutions at −30 °C.

Complexes **2a** and **2b** are thermally quite robust and melt at 122–124 °C and 112–114 °C, respectively. These compounds are monomeric in solid state and gas phase and can be sublimed in diffusion pump vacuum at 60–70 °C. However, the $^1$H NMR spectra of **2a** and **2b** in $C_6D_6$ and $C_4D_8O$ are distinctly different from those of $[(C_5Me_5)FeN(SiMe_3)_2]$, for which a spin state change has been observed in solution depending on the solvent.[31] Complexes **2a** and **2b** contain high spin iron(II) centers with four unpaired electrons ($S$ = 2) as determined by solution magnetic susceptibility studies yielding magnetic moments of 5.4(2) $\mu_B$ and 5.3(2) $\mu_B$, respectively, at 290 K independent of solvent, and exhibit well-resolved paramagnetic chemical shifts in the range +100 to −40 ppm (see Supporting Information, Table S1, and Experimental Section for details). In general, $^1$H NMR spectroscopy of paramagnetic mono(cyclopentadienyl) iron complexes is a very useful tool to distinguish monomeric from dimeric/trimeric species since they exhibit very distinct chemical shift patterns (Supporting Information, Table S1).

As expected for isostructural molecules **2a** and **2b** exhibit very similar temperature dependences of the chemical shifts (Figure 1). However, there is a slight curvature to the temperature dependence of the chemical shifts corresponding to the Cp′-*t*Bu groups especially at low temperatures. The nonlinearity of the $\delta$ vs $T^{-1}$ (Figure 1) might be caused by a hindered rotation of the Cp′-ring because of the sterically demanding $N(SiMe_3)(R)$ groups, and **2b** is ideal to evaluate this hypothesis. As a result of fast (on the NMR times scale)

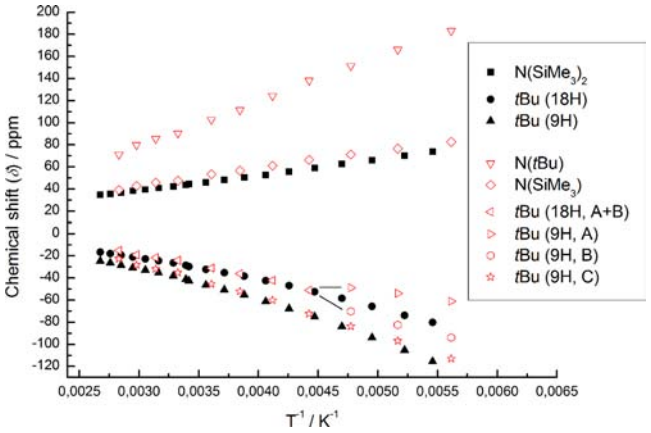


**Figure 1.** Chemical shift ($\delta$) vs $T^{-1}$ plot for **2a** and **2b**.

rotation along the Cp′(cent)–Fe and Fe–N axis the $^1$H NMR spectrum of **2b** is consistent with a time-averaged $C_s$ symmetry at ambient temperature (Chart 1). Decreasing the temperature

**Chart 1**

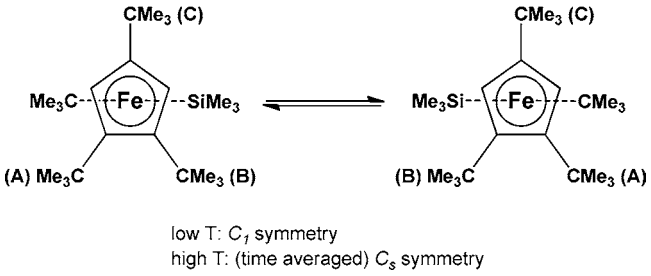


slows this rotation, and the two *t*Bu groups (A and B) undergo decoalescence (Figure 1) with a barrier of $\Delta G^{\ddagger}(T_c = -55\ ^\circ C)$ = 8 kcal/mol is derived for this process.

In an attempt to evaluate the relative binding strength of $[N(SiMe_3)(CMe_3)]^-$ and $[N(SiMe_3)_2]^-$ to the $[Cp'Fe]^+$ fragment a $C_6D_6$ solution of **2a**, **2b**, $[Li\{N(SiMe_3)(CMe_3)\}(OEt_2)]_2$ and $[Li\{N(SiMe_3)_2\}(OEt_2)]_2$ was transferred in an NMR tube. No exchange on the NMR time scale was observed, but when this mixture was heated at 65 °C for 25 days and equilibrium was established with $K_{eq}$ = 1.6(4) (Scheme 2). Hence there is a slight thermodynamic preference of the $[Cp'Fe]^+$ fragment for the more nucleophilic $[N(SiMe_3)(CMe_3)]^-$ moiety.

However, complexes **2a** and **2b** are exceedingly sensitive toward oxygen and moisture, and the reaction of **2a** with stoichiometric quantities of $H_2O$ yielded the trimeric iron hydroxo complex $[Cp'Fe(\mu\text{-}OH)]_3$ (**3**) (Scheme 3).[47]

**Iron Phenoxides.** The reaction of **2a** with $H_2O$ was quite encouraging and motivated us to investigate other Brønsted acids such as sterically demanding phenol ($pK_a$ ca. 18) and amine derivatives ($PhNH_2$, $pK_a$ ca. 30; $Ph_2NH$, $pK_a$ ca. 25).[48]


dx.doi.org/10.1021/ic301770f | Inorg. Chem. 2012, 51, 11860–11872

**Scheme 2. Chemical Exchange between 2a, 2b, $[Li\{N(SiMe_3)(CMe_3)\}(OEt_2)]_2$, and $[Li\{N(SiMe_3)_2\}(OEt_2)]_2$**

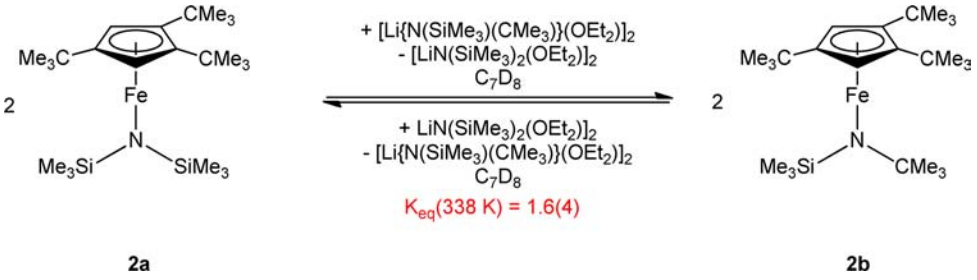


**Scheme 3. Reactivity of 2a with Various Brønsted Acids**

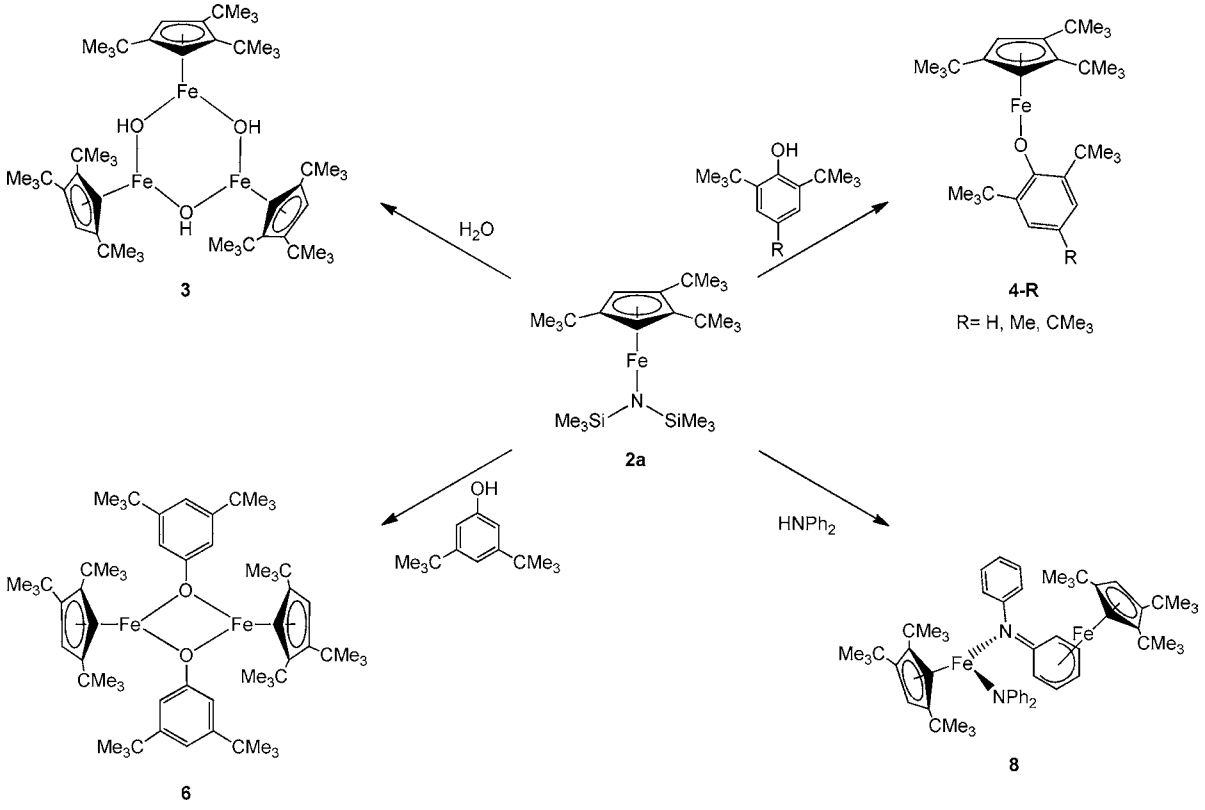


**Scheme 4. Rearrangement of 4-R to 5-R**

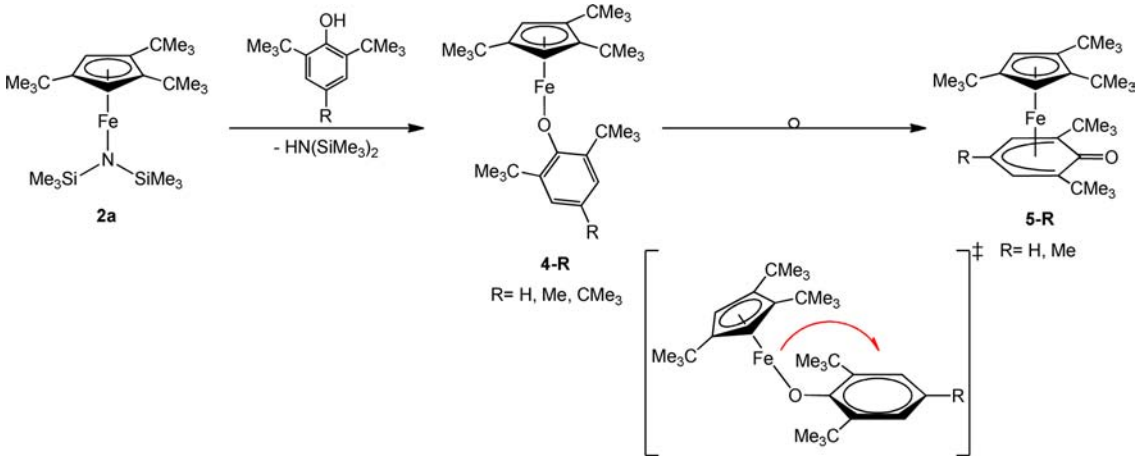


Complexes **2a** and **2b** should react with these more acidic substrates in an acid–base reaction, and this approach represents a synthetic alternative to a salt metathesis. Furthermore the starting materials and reaction products are (in most cases) soluble in $C_6D_6$, so the reaction progress can conveniently be monitored by NMR spectroscopy and the


dx.doi.org/10.1021/ic301770f | *Inorg. Chem.* 2012, 51, 11860–11872

**Table 1. Crystallographic Data**

| compound | **4-CMe$_3$** | **5-Me** | **6** | **8** | **9** |
|---|---|---|---|---|---|
| chemical formula | $C_{35}H_{59}FeO$ | $C_{32}H_{52}FeO$ | $C_{62}H_{100}Fe_2O_2$ | $C_{58}H_{78}Fe_2N_2$ | $C_{24}H_{48}FeSi_2$ |
| formula mass | 551.67 | 508.59 | 989.12 | 914.92 | 448.65 |
| crystal system | monoclinic | monoclinic | monoclinic | monoclinic | monoclinic |
| $a$/Å | 21.309(4) | 12.6864(4) | 11.1695(5) | 10.9446(2) | 9.8466(10) |
| $b$/Å | 16.214(3) | 15.0289(4) | 14.3936(6) | 38.0888(7) | 14.7897(16) |
| $c$/Å | 9.5786(16) | 15.2002(4) | 19.9752(8) | 13.1366(2) | 18.8919(19) |
| $\alpha$/deg | 90.00 | 90.00 | 90.00 | 90.00 | 90.00 |
| $\beta$/deg | 92.013(5) | 97.573(2) | 93.7720(10) | 113.7010(10) | 94.933(6) |
| $\gamma$/deg | 90.00 | 90.00 | 90.00 | 90.00 | 90.00 |
| unit cell volume/Å$^3$ | 3307.4(10) | 2872.83(14) | 3204.4(2) | 5014.32(15) | 2741.0(5) |
| temperature/K | 100(2) | 100(2) | 100(2) | 100(2) | 100(2) |
| space group | *C*2/*m* | *P*2(1)/*n* | *P*2(1)/*n* | *P*2(1)/*c* | *P*2(1)/*c* |
| no. of formula units per unit cell, $Z$ | 4 | 4 | 2 | 4 | 4 |
| radiation type | MoK$\alpha$ | MoK$\alpha$ | MoK$\alpha$ | CuK$\alpha$ | CuK$\alpha$ |
| absorption coefficient, $\mu$/mm$^{-1}$ | 0.479 | 0.546 | 0.488 | 4.915 | 5.272 |
| no. of reflections measured | 9845 | 40816 | 18861 | 72431 | 35321 |
| no. of independent reflections | 3060 | 8759 | 9281 | 9264 | 5039 |
| $R_{int}$ | 0.0666 | 0.0662 | 0.0325 | 0.0499 | 0.0540 |
| final $R_1$ values ($I > 2\sigma(I)$) | 0.0603 | 0.0425 | 0.0491 | 0.0443 | 0.0340 |
| final $wR(F^2)$ values ($I > 2\sigma(I)$) | 0.1561 | 0.0913 | 0.1307 | 0.1035 | 0.1048 |
| final $R_1$ values (all data) | 0.0924 | 0.0674 | 0.0708 | 0.0495 | 0.0415 |
| final $wR(F^2)$ values (all data) | 0.1694 | 0.1022 | 0.1399 | 0.1057 | 0.1193 |
| goodness of fit on $F^2$ | 1.081 | 1.025 | 1.052 | 1.142 | 1.061 |

stability of in situ generated species can be evaluated. The reaction of **2a** with substituted phenols is instantaneous, and the solution color changes immediately. NMR spectroscopy indicates the formation of monomeric or dimeric phenoxo complexes depending on the substitution pattern of the phenols (Scheme 3). Monomeric $\kappa^1$-*O* 14VE species are initially formed when the 2,6-positions of the phenols are blocked by sterically demanding $CMe_3$-groups that prevent dimer formation. However, the stability of these monomeric [Cp′FeOR] complexes is very sensitive toward the *para*-substitution at the phenol (Scheme 4): While in all cases, R = H, Me, and $CMe_3$, the monomeric 14VE [Cp′FeOR] complexes are initially formed (as confirmed by a similar solution VT-NMR behavior; see Supporting Information, Figures S1−S4 for details), *only* in the case of R = $CMe_3$ can the one-legged piano stool actually be successfully isolated. It is noteworthy that no significant spin-density is transferred to the *para*-position of the phenoxo ligand, since *p*-H and *p*-Me substituted derivatives exhibit the same temperature dependence, that is, the dipolar contributions to the chemical shift dominate the Fermi-contact terms.[49]

The formation of either $\kappa^1$-*O* or $\eta^5$-oxocyclohexadienyl coordination has previously been observed for iron half-sandwich complexes,[26] but it was not clear from these studies if a monomeric $\kappa^1$-*O* complex precedes the formation of the $\eta^5$-oxocyclohexadienyl compound, for example, for ruthenium it is postulated that the dimeric complex $[(C_5Me_5)Ru(\mu\text{-OR})]_2$ is involved in the rearrangement.[19,50] However, in our case the one-legged piano stools **4-H/Me** rearrange in solution and in solid state to form the diamagnetic oxocyclohexadienyl complexes **5-H/Me** (Scheme 4). While the rearrangement in solid state is not very clean and also significant amounts of insoluble material are obtained, this transformation is clean in solution and accompanied by a color change from orange-red to purple. The conversions of **4-H/Me** → **5-H/Me** were also followed by $^1$H NMR spectroscopy and found to obey first-order kinetics with similar activation barriers $\Delta G^{\ddagger}$(312 K) = 23.4(1) (R = H) and 23.7(1) (R = Me) kcal mol$^{-1}$ (see Experimental Section and Supporting Information for details). The slightly increased barrier for **4-Me** compared to **4-H** may be caused by steric rather than electronic effects.[51]

The monomeric **4-CMe$_3$** and the rearranged oxocyclohexadienyl sandwich complexes, **5-H/Me** (see Experimental Section for details) were isolated, and the molecular structures of **4-CMe$_3$** and **5-Me** were determined by single crystal X-ray diffraction (Table 1, Figures 2 and 3). Selected bond distances and angles are given in the Figure captions. The long Fe-Cp(cent) distance of 1.88 Å in **4-CMe$_3$** is comparable to the ones observed for **1** (1.93 Å),[45] **2a-DMAP** (2.05 Å),[47] **3** (1.97 Å),[47] and $[(C_5Me_5)FeN(SiMe_3)_2]$ (1.90 Å).[31] It is indicative of a high spin Fe(II) center ($S$ = 2) and can be compared to ca.

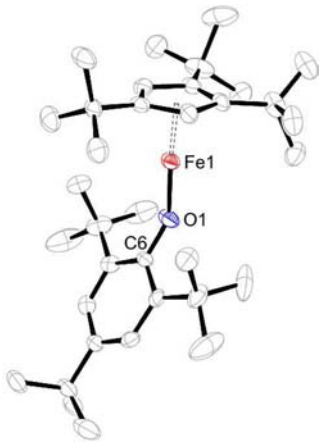


**Figure 2.** ORTEP diagram of **4-CMe$_3$** (ellipsoids at 50% probability level). Selected bond distances (Å) and angles (deg): Cp(cent)−Fe1 1.88, Fe1−O1 1.811(4), O1−C6 1.345(6), Cp(Cent)−Fe1−O1 175.1, Fe1−O1−C6 144.0(3).


dx.doi.org/10.1021/ic301770f | *Inorg. Chem.* 2012, 51, 11860−11872

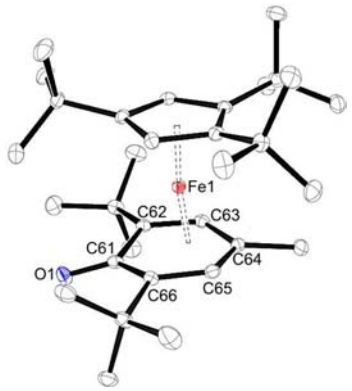


**Figure 3.** ORTEP diagram of **5-Me** (ellipsoids at 50% probability level). Selected bond distances (Å) and angles (deg): Cp(cent)−Fe1 1.72, Fe1−Cp(plane) 1.717, Fe1−dienyl(plane) 1.635, Fe1−C61 2.4421(15), Fe1−C62 2.2098(14), Fe1−C63 2.1029(14), Fe1−C64 2.1221(16), Fe1−C65 2.0988(16), Fe1−C66 2.2115(16), C61−O1 1.2478(19), C61−C62 1.469(2), C62−C63 1.414(2), C63−C64 1.407(2), C64−C65 1.411(2), C61−C66 1.472(2), ∠ Cp(plane)−dienyl(plane) 0.71.

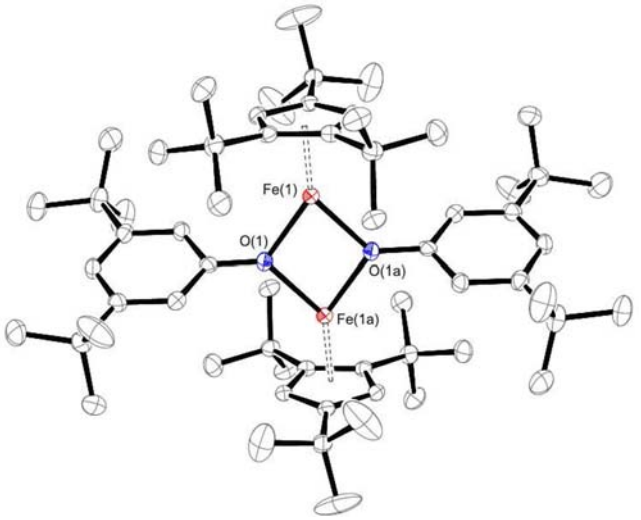


**Figure 4.** ORTEP diagram of **6** (ellipsoids at 50% probability level). Selected bond distances (Å) and angles (deg): Cp(cent)−Fe(1) 1.94, Fe(1)−O(1) 1.9881(12), Fe(1)−O(1a) 2.0115(13), Fe(1)···Fe(1a) 3.06, O(1)−Fe(1)−O(1a) 80.03(5), Fe(1)−O(1)−Fe(1a) 99.97(5).

1.7 Å for closed-shell ($S$ = 0) iron complexes such as **5-Me**, $[Cp'_2Fe]$,[45] and other iron half-sandwich complexes.[52] This notion is further supported by the solution magnetic susceptibility data for **4-CMe$_3$** of 5.3(2) $\mu_B$ (at 300 K).

However, when the $CMe_3$-groups are moved from the *ortho*-(2,6)- to the *meta*-(3,5)-positions the steric hindrance is no longer sufficient to stabilize a monomeric species, and the green dimer **6** is formed in good yield (Scheme 3). Because of the low solubility of **6** in aromatic and aliphatic solvents, the formation is rapid, and no intermediate (such as a monomeric [Cp′FeOR] species) was observed by NMR spectroscopy. Complex **6** is thermally quite robust (mp 218−221 °C (rev.)) and shows a molecular ion in the EI-MS spectrum. The solution magnetic moment of **6** was determined with the Evans method yielding a magnetic moment (per iron center at 290 K) of 5.5(2) $\mu_B$ (cf. $[Cp'FeI]_2$: 5.3(2) $\mu_B$).[45] No rearrangement at elevated temperature to an oxocyclohexadienyl complex or exchange with free phenol was observed in solution in contrast to $[(C_5Me_5)Ru(\mu\text{-}OR)]_2$.[19,50] Possible explanations for this reactivity difference may include the more sterically hindered environment at the Fe atom in **6**, the different spin states in both complexes and the reduced arenophilicity of the $[Cp'Fe]^+$ fragment[45] when compared to $[(C_5Me_5)Ru]^+$. The $\delta$ vs $T^{-1}$ plot is linear in the temperature range −100 °C to +100 °C and suggests that electron exchange coupling between the two Fe(II) ($S$ = 2) centers is small and that no dissociation of the $Fe_2O_2$ core into monomeric fragments occurs in solution (see Supporting Information, Figures S6 and S7 for details). Strong Fe−O bonds have also been observed for $[Fe(OC_6H_2tBu_3\text{-}2,4,6)_2]_2$.[35]

The solid state structure of **6** is shown in Figure 4, and selected bond distances and angles are given in the Figure caption. The two halves of the dimer are related by a center of symmetry. Thus the $Fe_2O_2$ core is required to be planar. The internal ring angle at the iron atom is 80.03(5)° and 99.97(5)° at the oxygen atom. Overall the structural features are related to $[Fe\{N(SiMe_3)_2\}\{\mu\text{-}OC_6H_2tBu_3\text{-}2,4,6\}]_2$.[35] The high spin configuration at the iron atom is reflected in the Cp(cent)−Fe distance of 1.94 Å.

**Iron Anilido.** Interestingly, whereas monomeric phenoxo systems using sterically encumbered phenols are readily available from **2a**, the analogue anilido species **7** must be synthesized by salt metathesis from **1** and $[Li(NHC_6H_2tBu_3\text{-}2,4,6)(OEt_2)]_2$. The origin of this reactivity difference is mainly due to steric reasons, since less encumbered aniline derivatives (such as *p*-toluidine) with similar p$K_a$ values yield dimeric complexes of two different isomers.[53] It is interesting to note that no reaction was observed between **2a** or **2b** with a bulky $\beta$-diketimine (Hnacnac = $H_2C\{C(Me)(2,6\text{-}i\text{-}Pr_2C_6H_3N)\}_2$) even at elevated temperatures (65 °C) for a prolonged period of time. In contrast, $[(nacnac)FeN(SiMe_3)_2]$ is accessible via acid−base reaction between Hnacnac and $[Fe\{N(SiMe_3)_2\}_2]_2$ at 110−120 °C under solvent-free conditions.[39] Unfortunately, no suitable single crystals for an X-ray diffraction experiment were obtained, but the VT-NMR study for $[Cp'FeNH(C_6H_2(CMe_3)_3\text{-}2,4,6)]$ (**7**) reveals a similar temperature dependence as the phenolate complex **4-CMe$_3$** which is expected for structurally related complexes (see Supporting Information, Figure S8 for details). The solution magnetic susceptibility data for **7** (5.3(2) $\mu_B$ at 298 K) further supports this notion. No resonances corresponding to the anilido NH and the Cp′ ring-CH protons were found in the $^1$H NMR spectrum presumably because of extreme line broadening. However, an N−H stretching vibration was observed at 3380 cm$^{-1}$ in the IR spectrum of **7**.

In general, amido transition metal complexes can be used for the synthesis of terminal imido complexes and two different strategies have been employed in this context: (a) concerted proton-coupled electron transfer (PCET) and (b) stepwise oxidation and proton abstraction. The PCET approach has precedence in the work by Hillhouse[54] and Smith.[55] Attempts to deprotonate **7** with $[LiN(SiMe_3)_2(OEt_2)]_2$ failed, and instead an equilibrium mixture of **2a**, **7**, and $[Li(NHC_6H_2(CMe_3)_3\text{-}2,4,6)(OEt_2)]_2$, and $[LiN(SiMe_3)_2(OEt_2)]_2$ is established in $C_6D_6$ solution, $K_{eq}$(298 K) = 34(2) (Scheme 5). This shows a slight thermodynamic preference of the $[Cp'Fe]^+$ fragment for the $[N(SiMe_3)_2]^-$ group compared to the $[NHC_6H_2(CMe_3)_3\text{-}2,4,6)]^-$ moiety. For comparison, no reaction was observed for $[(nacnac^{Me})Fe(NHtol)]$ ($nacnac^{Me}$ = $HC\{C(Me)(2,6\text{-}i\text{-}Pr_2C_6H_3N)\}_2$) and strong bases such as $LiN(SiMe_3)_2$ and NaO$t$Bu.[56] The lack of reactivity might


dx.doi.org/10.1021/ic301770f | Inorg. Chem. 2012, 51, 11860−11872

**Scheme 5. Synthesis and Reactivity of 7**

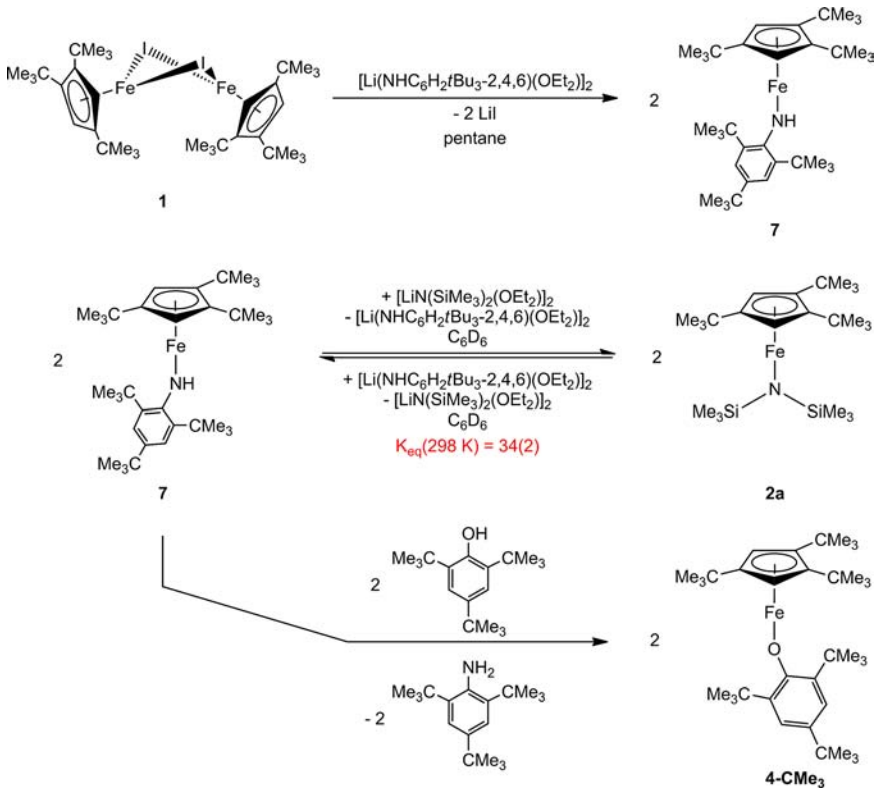


again be related to steric hindrance in the transition state of proton transfer. However, on addition of $HOC_6H_2(CMe_3)_3$-2,4,6 to **7** the monomeric iron phenoxo complex **4-CMe$_3$** was formed. Addition of $C_2H_4I_2$ leads to the formation of the unusual 15VE iron(III) half-sandwich complex [Cp′FeI$_2$].[57] Since this phenol can participate in a proton transfer reaction it is likely to assume that the stable supermesitylene phenoxo radical, $[2,4,6\text{-}(Me_3C)_3C_6H_2O]^{\bullet}$, might be suitable for a concerted PCET, and attempts in this directions are ongoing.

In contrast, **2a** reacts with $HNPh_2$ at elevated temperatures to a red crystalline compound that is nearly insoluble in aliphatic and aromatic hydrocarbons, but decomposes in $CH_2Cl_2$. Although $[PhB(CH_2PiPr_2)_3]^-$ and $[Cp']^-$ are isoelectronic, their reactivity with the $[Ph_2N]^-$ ligand differs distinctly. In the case of $[PhB(CH_2PiPr_2)_3]^-$ the monomeric high spin ($S$ = 2) iron amide complex [{$PhB(CH_2PiPr_2)_3$}Fe-($NPh_2$)] was isolated,[58] whereas [Cp′Fe($N,C$-$\kappa^1,\eta^5$-$C_6H_5NPh$)-Fe($N$-$\kappa^1$-$NPh_2$)Cp′] (**8**) is formed with Cp′ in which a cationic [Cp′Fe]$^+$ fragment coordinates to an anionic *N,N*-phenyl-cyclohexadienyl-imine ligand, and a neutral [Cp′Fe$NPh_2$] fragment is coordinated to the imino functionality (Scheme 3 and Figure 5). For comparison the homoleptic dimer [Fe($NPh_2$)$_2$]$_2$ shows Fe−N distances of 1.895(3) and 2.036(3) Å for the terminal and bridging $NPh_2$ groups, respectively.[59] More importantly, **8** combines in one molecule two iron centers in the same oxidation state (+2), but different spin-states ($S$ = 0 and $S$ = 2) which is nicely reflected in very different Cp(cent)−Fe distances of 1.68 and 2.04 Å, respectively. Only one other complex was reported that contains a comparable structural feature. In this case a lithium ion is coordinated to the O-donor atoms of a bis($\mu,\kappa$-*O*-2,6-dimethylphenolato)(tetraisopropylcyclopentadienyl)ferrate(II)-ion and the oxocyclohexadienyl of an iron sandwich complex.[26]

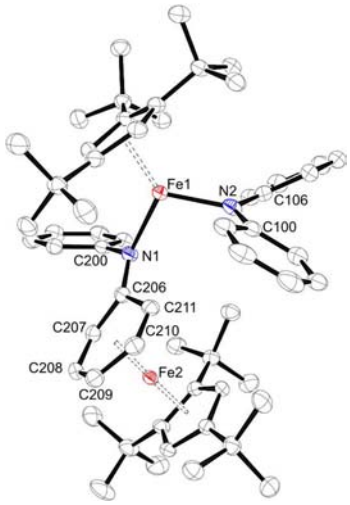


**Figure 5.** ORTEP diagram of **8** (ellipsoids at 50% probability level). Selected bond distances (Å) and angles (deg): Cp(cent)−Fe1 2.04, Cp(plane)−Fe1 2.036, Cp(cent)−Fe2 1.68, Cp(plane)−Fe2 1.683, Fe1−N1 2.1494(18), N1−C200 1.436(3), N1−C206 1.333(3), Fe1−N2 2.047(2), N2−C100 1.387(3), N2−C106 1.398(3), C206−C207 1.441(3), C207−C208 1.414(3), C208−C209 1.406(3), C210−C211 1.409(3), C211−C206 1.434(3), Fe2-dienyl(plane) 1.563, Fe2−C206 2.427(2), Fe2−C207 2.124(2), Fe2−C208 2.054(2), Fe2−C209 2.076(2), Fe2−C210 2.060(2), Fe2−C211 2.128(2), ∠ Cp(plane)−dienyl(plane) 1.89.

However, a similar rearrangement from an amido to an imino ligand was observed by Hillhouse for a [(NHC)Ni-($NHC_6H_3(iPr)_2$-2,6)] (NHC = N-hetereocyclic carbene) upon oxidation.[60] Unfortunately, the slow reaction and the lack of solubility of **8** make it difficult to elucidate the reaction


dx.doi.org/10.1021/ic301770f | *Inorg. Chem.* 2012, 51, 11860−11872

**Scheme 6. Synthesis and Reactivity of 9**

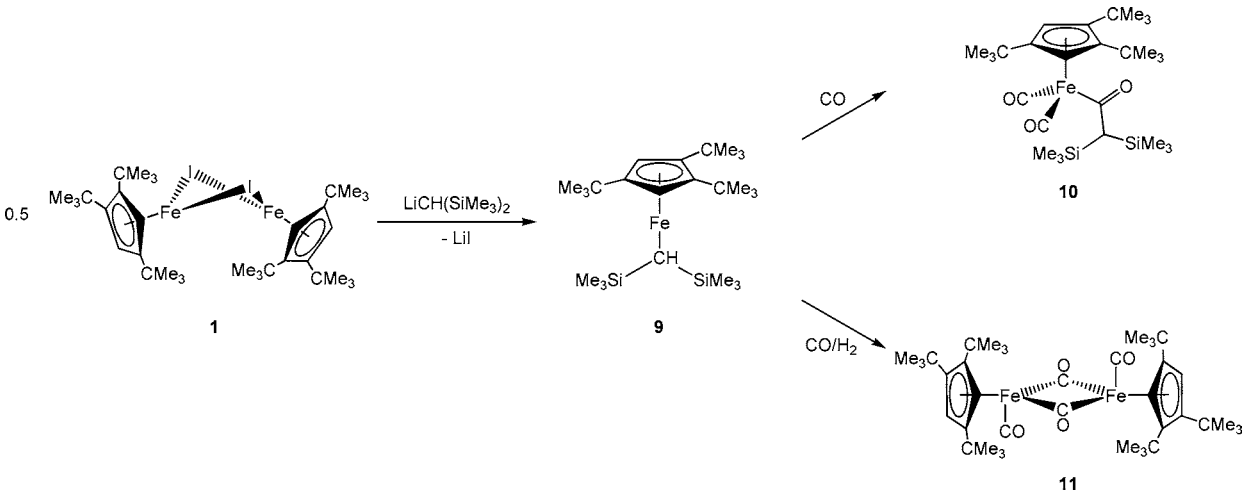


mechanism, for example, to confirm the initial formation of a one-legged piano stool vs dimeric complex or to obtain any kinetic information on this rearrangement process.

**Iron Alkyls.** Two alternative entries into the synthesis of "Cp′FeH" complexes can be considered either by hydrogenation of a "Cp′FeR" precursor or salt methathesis of **1** with $KHBEt_3$. Both approaches have precedents in the work by Peters and Holland for the synthesis of low-coordinate Fe−H molecules. Peters and co-workers demonstrated that a $[\{PhB(CH_2PiPr_2)_3\}FeMe]$ complex can react in the presence of a suitable phosphine trap to generate $[\{PhB(CH_2PiPr_2)_3\}Fe(H)(PMe_3)]$ and $[\{PhB(CH_2PiPr_2)_3\}Fe(H)_3(PMe_3)]$, respectively, while in the absence of such traps the iron hydride reacts with aromatic solvents to form cyclohexadienyl-capped Fe(II) complexes.[61,62] In contrast, Holland and co-workers showed that despite the fact that [(nacnac)Fe-R] species (nacnac = $HC\{C(CMe_3)(2,6\text{-}i\text{-}Pr_2C_6H_3N)\}_2$) are accessible and have also a $S = 2$ ground state like the phosphinoborate complex, the nacnac complexes do not react with $H_2$, but under an atmosphere of CO insertion into the Fe-R bond occurs.[63] However, we have previously reported on the reactivity of **1** with $KHBEt_3$ and showed that initially formed "Cp′FeH" species is unstable and degrades to $[Cp'_2Fe_2H_3]$ and $[Cp'FeH_2]_2$ under an argon atmosphere, while in the presence of $H_2$ the formation of $[Cp'FeH_2]_2$ becomes more favorable.[46] Here, we want to investigate mono(cyclopentadienyl) iron alkyl complexes and their reactivity toward small molecules. Several attempts to react **1** and MeLi to prepare a stable "[Cp′FeMe]" derivative failed and only the cleavage of the Cp′Fe-fragment accompanied by the formation of $[Li(OEt_2)][Cp']$ was detected. This is in agreement with previous reports that showed that Cp′ is not inert to substitution when reacted with organolithium reagents.[64,65]

However, the use of a sterically more demanding alkyl group such as $LiCH(SiMe_3)_2$ allowed the isolation of the monomeric 14VE complex, $[Cp'FeCH(SiMe_3)_2]$ (**9**) (Scheme 6). Complex **9** is soluble in all common organic solvents, and thermally quite robust. No degradation occurred when **9** was heated in $C_6D_6$ solution at 65 °C for 30 days, while its stability in solid state was exemplified by reversible melting point behavior, and on sublimation under diffusion pump vacuum at 60−65 °C. In addition, a molecular ion of **9** is observed in the EI-MS spectrum ($[M^+]$ = 448 amu). As expected, **9** is exceedingly sensitive to trace amounts of moisture and oxygen. The Evans' moment in solution of $\mu_{eff}(292\ K) = 5.0(2)\ \mu_B$ confirms the high spin configuration with 4 unpaired spins ($S = 2$). Variable temperature $^1H$ NMR studies for **9** were undertaken and a deviation from linearity in the $\delta$ vs $T^{-1}$ plot was noted (Figure 6). We attribute this observation to a hindered rotation of the

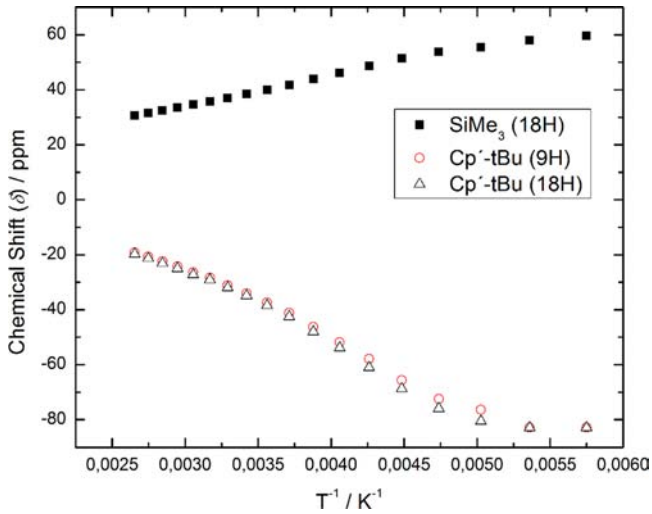


**Figure 6.** Chemical shift ($\delta$) vs $T^{-1}$ plot for **7**.

Cp′ fragment relative to the bulky alkyl group changing the dipolar contribution to the chemical shift.[49] However, the barrier is relatively low, and no decoalescence behavior was observed. An ORTEP diagram of **9** is shown in Figure 7, and selected bond distances and angles are given in the figure caption. The molecular structures of $[^nCpFe(\sigma\text{-}C_6H_3iPr_2\text{-}2,6)]$ ($^nCp$ = $^4Cp$[29] and $^5Cp$[30]) were reported, and the metric parameters agree well with those presented in this work.

Despite the high reactivity of **9** toward trace amounts of oxygen and moisture, it proved to be surprisingly unreactive. No reaction was observed with $N_2O$ (1 atm), $C_2H_4$ (1 atm), or $H_2$ (1 atm) at ambient temperature even after 7 days. Since the reaction of **9** with $H_2$ is formally spin-forbidden several attempts to induce a spin-state change at room temperature have been undertaken, for example, on addition of a good $\sigma$-donating ligand such as 4-*N*,*N*-dimethylaminopyridine (DMAP) in the presence of $H_2$. While in the presence of an


dx.doi.org/10.1021/ic301770f | Inorg. Chem. 2012, 51, 11860−11872

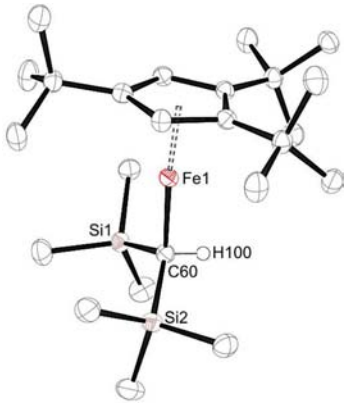


**Figure 7.** ORTEP diagram of [Cp′FeCH(SiMe$_3$)$_2$] (ellipsoids at 50% probability level). The hydrogen atom on C60 was located in the Fourier difference map and refined isotropically. Selected bond distances (Å) and angles (deg): Cp(cent)−Fe(1) 1.91, C(60)−Si(1) 1.8680(19), C(60)−Si(2) 1.8651(18), Fe(1)−C(60) 2.035(2), C(60)−H(100) 0.93(3), Cp(cent)−Fe(1)−C(60) 172.8. No short contacts or agostic bonds are observed in the crystal structure.

excess of DMAP a mono-DMAP adduct, **9*(DMAP)** is formed, rapid exchange between free and bound DMAP was observed on the NMR time scale. This behavior is reminiscent of the weak DMAP adduct to **2a**, **2a*(DMAP)**.[47] However, no reaction with $H_2$ was detected suggesting that DMAP binding is weak and does not induce the necessary spin-state change to facilitate the hydrogenolysis of the Fe-alkyl bond. Overall, **9** behaves analogous to the 12VE [(nacnac)FeR] systems.[63] The influence of spin-states on reaction mechanisms and rate constants has been subject to intense debates over the years. However, there has been a growing number of examples and computational studies supporting the notion that spin-states can indeed affect the reaction rate.[66,67] This was exemplified by the slow addition of $H_2$ to [W{N(CH$_2$CH$_2$NSiMe$_3$)$_3$}H] which is a "spin-blocked" reaction with a high reaction barrier due to crossing between the reactant triplet and the product singlet potential energy surfaces.[68]

Hence, the reactivity of **9** toward a good $\pi$-acceptor ligand such as CO and a CO/$H_2$ mixture (ratio 30:70) was investigated. The reaction of **9** in pentane solution under CO (1 atm) proceeds smoothly to give the iron acyl-complex [Cp′Fe(CO)$_2$(C(O)CH(SiMe$_3$)$_2$] (**10**). The presence of a $\kappa^1$-acyl coordination mode (instead of $\eta^2$-acyl) is verified by the $^{13}$C{$^1$H} NMR data. Crystals of moderate quality were grown from concentrated hexamethyldisiloxane solution at −38 °C. Although the quality of the structure precludes a detailed discussion of bond distances and angles, the connectivity was clearly established and a ball-stick representation of **10** is shown in Supporting Information, Figure S11. Complex **10** is a rare example of CO insertion into a M-CH(SiMe$_3$)$_2$ moiety, but it has been observed for group 4 transition metal complexes.[69]

The reaction of **10** with a mixture of CO and $H_2$ (30:70) at ambient temperature proceeds differently. While CH$_2$(SiMe$_3$)$_2$ was detected as one of the side products of this transformation, the only isolated product was the known carbonyl complex [Cp′Fe(CO)$_2$]$_2$ (**11**).[70] This implies that the hydrogenolysis of the Fe-R bond is feasible in the presence of a good $\pi$-acceptor ligand such as CO which induces the required spin-state change for the reaction with $H_2$ to proceed. However, the reaction mechanism and the intermediacy of other species such as an iron formyl-complex are subject to further investigations at low temperature and will be reported in due course.

## COMPUTATIONAL RESULTS

Density functional theory (DFT) calculations in concert with experimental data have become valuable tools in organometallic chemistry. Especially for larger molecules and clusters of low symmetry, the low computational expense compared to post-Hartree−Fock methods makes DFT very often the only option when the electronic structure of complex systems needs to be evaluated. However, the exact functional of the electron density is unknown and only approximate expressions are available; hence an exhaustive evaluation of different Density Functionals (DFs) is required. We have previously evaluated a series of modern hybrid and hybride meta DFs and found that the best agreement between experimental and calculated structures have been achieved with the dispersion-corrected B97 functional, B97D[71] in combination with the 6-311G(d,p) basis set.[46,52] Encouraged by this previous success we investigated computationally selected complexes for which structural and magnetic data were available at the B97D/6-311G(d,p) level of theory and found that the computed geometries of these complexes agree very well with the experimental X-ray diffraction data (see Supporting Information, Table S2 for details). We also extended our computational study to molecules for which no structural data were available and addressed the question of spin states and relative energy of these spin states (Figure 8 and

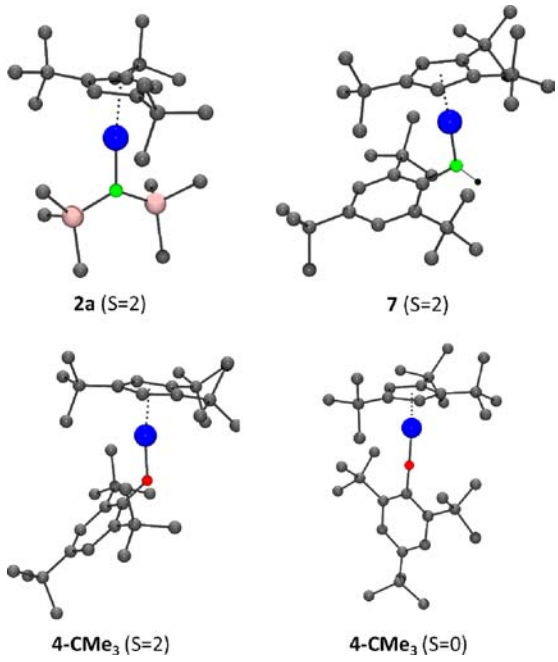


**Figure 8.** Calculated structures for several iron one-legged piano stools.

see Supporting Information for details). For [(C$_5$Me$_5$)FeN(SiMe$_3$)$_2$] a low and high spin state was observed depending on the solvent.[31] In contrast for **2a** the high spin state prevails in solid state and solution independent of solvent.[47] Calculations at the B97D/6-311G(d,p) level of theory also favor the high spin state for **2a** by $\Delta G$(298 K) = 12.1 kcal/mol in agreement with the experimental data. The related alkyl **9** and phenoxo complexes **4-CMe$_3$** exhibit a similar stabilization of the high


dx.doi.org/10.1021/ic301770f | Inorg. Chem. 2012, 51, 11860−11872

spin state with $\Delta G(298\ K) = 17.3$ and 9.8 kcal/mol, respectively.

The next question of interest was the relative bond strength of Fe−N(SiMe$_3$)$_2$ vs Fe-NHR and Fe-OR bonds. From the experiments discussed above the following relative order is expected Fe-OR ≫ Fe−N(SiMe$_3$)$_2$ ≥ Fe-NHR and DFT calculations predict the following free enthalpies ($\Delta G$):

**2a** + HOC$_6$H$_2$*t*Bu$_3$-2,4,6 → **4-CMe$_3$** + HN(SiMe$_3$)$_2$;

$\Delta G(298\ K) = -16.7$ kcal/mol

**2b** + HOC$_6$H$_2$*t*Bu$_3$-2,4,6 → **4-CMe$_3$** + HN(SiMe$_3$)(CMe$_3$);

$\Delta G(298\ K) = -18.1$ kcal/mol

**9** + HOC$_6$H$_2$*t*Bu$_3$-2,4,6 → **4-CMe$_3$** + H$_2$C(SiMe$_3$)$_2$;

$\Delta G(298\ K) = -28.6$ kcal/mol

**2a** + H$_2$NC$_6$H$_2$*t*Bu$_3$-2,4,6 → **7** + HN(SiMe$_3$)$_2$;

$\Delta G(298\ K) = -4.5$ kcal/mol

**2b** + H$_2$NC$_6$H$_2$*t*Bu$_3$-2,4,6 → **7** + HN(SiMe$_3$)(CMe$_3$);

$\Delta G(298\ K) = -5.9$ kcal/mol

**9** + H$_2$NC$_6$H$_2$*t*Bu$_3$-2,4,6 → **7** + H$_2$C(SiMe$_3$)$_2$;

$\Delta G(298\ K) = -16.4$ kcal/mol

**7** + HOC$_6$H$_2$*t*Bu$_3$-2,4,6 → **4-CMe$_3$** + H$_2$NC$_6$H$_2$*t*Bu$_3$-2,4,6;

$\Delta G(298\ K) = -12.2$ kcal/mol

On the basis of these results the reaction of **2a**/**2b** with H$_2$NC$_6$H$_2$(CMe$_3$)$_3$-2,4,6 is slightly exergonic and should proceed at room temperature. While there is a methodological uncertainty associated with DFT methods and open-shell systems, which is usually on the order of a few kcal/mol, the predicted trends are generally correct. In addition, we attribute the experimentally observed lack of reactivity to the steric hindrance at the metal center which prevents efficient proton transfer in the transition state. This is consistent with the experimental fact that the reaction proceeds with less substituted aniline derivatives. In these cases an additional driving force is provided by the formation of dimeric $\mu$-anilido complexes. For [Cp′Fe($\mu$-OC$_6$H$_3$*t*Bu$_2$-3,5)]$_2$ (**6**) the dimerization of two monomeric [Cp′Fe($\mu$-OC$_6$H$_3$*t*Bu$_2$-3,5)] ($S = 2$) fragments is quite exergonic with $\Delta G^0(298\ K) = -34.5$ kcal/mol (see Supporting Information for details).

We also evaluated the energetics for the transformation **4-R** → **5-R** in which sterically encumbered groups in the *para*-position of the phenolate ligand prevent this rearrangement. Figure 9 shows the Gibbs free energy profile. The calculations are in good qualitative agreement with the experiments, for example, the transition states connecting **4-R** ($S = 2$) → **5-R** ($S = 2$) react sensitive to the *para*-substitution. The transition state converting **5-R** ($S = 2$) → **5-R** ($S = 0$) has not been located, but the additional intersystem crossing barrier is most likely responsible for the larger barrier ($\Delta G^{\ddagger}$ = ca. 23 kcal/mol) observed experimentally. However, as a results of steric repulsion the final products **5-R** ($S = 0$) differ significantly in their thermodynamic stability compared to the starting materials **4-R** ($S = 2$), for example, the reaction is close to thermoneutrality for R = CMe$_3$ whereas the reaction is exergonic for R = H and Me substitution.[72]

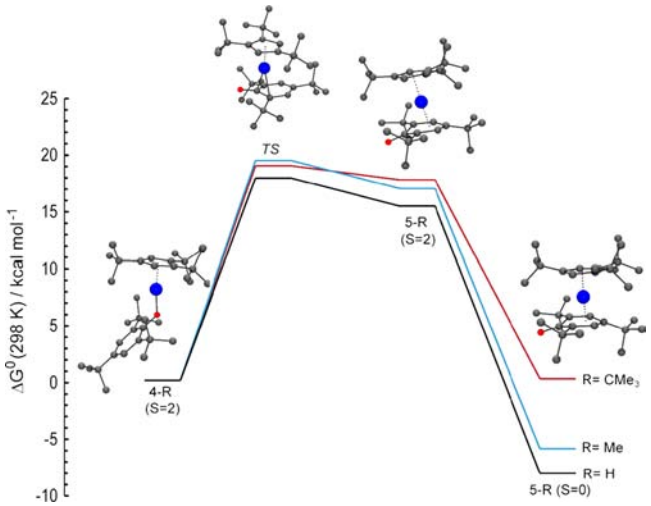


**Figure 9.** Free energy diagram, $\Delta G^0(298\ K)$, for the rearrangement **4-R** → **5-R**.

## CONCLUSIONS

The one-legged piano stool iron amido complexes [Cp′Fe{N(SiMe$_3$)(R)}] (R = SiMe$_3$ (**2a**) and CMe$_3$ (**2b**)) are excellent starting materials for salt-free metathesis reactions with more acidic substrates. However, the outcome of the reaction is determined by the steric demand of the phenols, and monomeric and dimeric phenoxo complexes are formed. In the case of 2,6-di-*t*-butyl substituted phenols paramagnetic monomeric complexes (**4-R**) are initially observed which rearrange to diamagnetic oxocyclohexadienyl complexes (**5-R**) when the 4-position carries an H or a Me group. However, *t*Bu-substitution in 4-position stabilizes the one-legged piano stool fragment. Alternatively, 3,5-di-*t*-butyl substituted phenol yields a paramagnetic (monocyclopentadienyl) iron phenoxo dimer [Cp′Fe($\mu$-OC$_6$H$_3$*t*Bu-3,5)]$_2$ (**6**). With aniline derivatives the reaction is less straightforward and the one-legged piano stool anilido complex [Cp′Fe(NHC$_6$H$_2$*t*Bu$_3$-2,4,6)] (**7**) is not accessible via acid−base reaction, but can be prepared by conventional salt metathesis. In contrast, reaction of **2a** with Ph$_2$NH yields the bimetallic [Cp′Fe(*N*,*C*-$\kappa^1$,$\eta^5$-C$_6$H$_5$NPh)Fe(*N*-$\kappa^1$-NPh$_2$)Cp′] (**8**) which combines two iron centers in the same oxidation state (+2), but different spin-states ($S = 0$ and $S = 2$). An alkyl iron one-legged piano stool [Cp′FeCH(SiMe$_3$)$_2$] (**9**) can be prepared, but despite being low-coordinate and possessing only 14VE no reactivity was observed with ethylene, N$_2$O or H$_2$ even at elevated temperatures. This behavior is most likely traced to a spin-state introduced reaction barrier which precludes the reaction between the high-spin iron center and the closed shell substrate. In the presence of strong field ligands such as CO or CO/H$_2$ mixtures the iron(II) acyl complex [Cp′Fe(CO)$_2$(C(O)CH(SiMe$_3$)$_2$)] (**10**) and the iron(I) carbonyl [Cp′Fe(CO)$_2$]$_2$ (**11**) are formed, respectively.

Additional reactivity studies and the quest for iron multiple-bonded species are ongoing and will be reported in due course. In addition we are currently investigating the issue of spin-state induced reaction barriers in these mono(cyclopentadienyl) iron complexes and the consequences thereof.


dx.doi.org/10.1021/ic301770f | *Inorg. Chem.* 2012, 51, 11860−11872

## EXPERIMENTAL SECTION

**General Considerations.** All reactions and product manipulations were carried out under an atmosphere of dry, oxygen free argon or dinitrogen using standard high-vacuum, Schlenk, or drybox techniques. Argon was purified by passage through BASF R3-11 catalyst (Chemalog) and 4 Å molecular sieves. Dry, oxygen-free solvents were employed throughout. NMR spectra were recorded on Bruker DRX 500 MHz, a Bruker DRX 400 MHz, or a Bruker 400 MHz AVANCE spectrometer. All chemical shifts are reported in $\delta$ units with reference to the residual protons of the deuterated solvents, which are internal standards, for proton chemical shifts. Probe temperatures were calibrated using ethylene glycol and methanol as previously described.[73] The elemental analyses were performed by the analytical facilities at the University of California at Berkeley or at the TU Braunschweig. Crystallographic data were also deposited with Cambridge Crystallographic Data Centre. Copies of the data (CCDC 893606−893610) can be obtained free of charge via http://www.ccdc.cam.ac.uk/data_request/cif by e-mailing data_request@ccdc.cam.ac.uk, or by contacting The Cambridge Crystallographic Data Centre, 12, Union Road, Cambridge CB 1EZ, U.K.; fax +44 1223 336033.

**Materials.** All solvents were deoxygenated and dried by passage over columns of activated alumina.[74] Tetrahydrofuran was dried over sodium/benzophenone and freshly distilled prior to use. Deuterated solvents, $CD_2Cl_2$, $C_6D_6$, $C_7D_8$, cyclohexane-$d_{12}$ and methylcyclohexane-$d_{14}$, were purchased from Cambridge Laboratories, Inc., refluxed for 3 days over sodium metal (with the exception of $CD_2Cl_2$ which was dried over $CaH_2$ for 4 days), vacuum transferred to a Teflon sealable Schlenk flask containing 4 Å molecular sieves, and degassed via three freeze−pump−thaw cycles. $[Cp'FeI]_2$, $[Li(NHC_6H_2tBu_3\text{-}2,4,6)(OEt_2)]_2$, $[LiCH(SiMe_3)_2]$, and $[Li\{N(SiMe_3)(CMe_3)\}(OEt_2)]_2$ were prepared according to literature procedures.[45,75−77]

All other chemicals were purchased from Acros Organics or Sigma Aldrich. The substituted phenols and aniline derivatives were sublimed prior to use. The solution magnetic susceptibility was determined using a modified[78] Evans method.[79]

**Synthesis.** *[Cp′FeN(SiMe$_3$)$_2$] (**2a**).*[47] A mixture of $[Cp'FeI]_2$ (**1**) (1.41 g, 1.7 mmol) and $[Li\{N(SiMe_3)_2\}(OEt_2)]_2$ (0.81 g, 3.4 mmol) was dissolved in about 20 mL of pentane, and the reaction mixture turned immediately bright yellow. The solution was stirred for 10 min and filtered. The solvent was removed under reduced pressure, and the yellow residue was sublimed in diffusion pump vacuum at 60−70 °C to give yellow crystalline material (1.06 g, 2.36 mmol, 69%). Mp 122−124 °C (rev.). $^1$H NMR ($C_6D_6$, 292K): $\delta$ 44.9 (18H, $SiMe_3$, $\nu_{1/2}$ = 1100 Hz), −30.3 (18H, $CMe_3$, $\nu_{1/2}$ = 1050 Hz), −42.6 (9H, $CMe_3$, $\nu_{1/2}$ = 700 Hz). $^1$H NMR (thf-$d_8$, 292K): $\delta$ 43.8 (18H, $SiMe_3$, $\nu_{1/2}$ = 690 Hz), −29.0 (18H, $CMe_3$, $\nu_{1/2}$ = 700 Hz), −41.6 (9H, $CMe_3$, $\nu_{1/2}$ = 570 Hz). $^1$H NMR (py-$d_5$, 292K): $\delta$ 18.3 (18H, $SiMe_3$, $\nu_{1/2}$ = 640 Hz), −13.6 (18H, $CMe_3$, $\nu_{1/2}$ = 430 Hz), −24.1 (9H, $CMe_3$, $\nu_{1/2}$ = 540 Hz). $^1$H NMR ($CD_2Cl_2$, 292K): $\delta$ 43.5 (18H, $SiMe_3$, $\nu_{1/2}$ = 980 Hz), −29.2 ppm (18 H, Cp′-$CMe_3$, $\nu_{1/2}$ = 900 Hz), −42.0 ppm (9 H, Cp′-$CMe_3$, $\nu_{1/2}$ = 630 Hz). IR (Nujol mull; CsI windows; cm$^{-1}$): 1365m, 1260m, 1249vs, 1205vw, 1160vw, 1100vbr.vw., 1005sh, 970brvs, 875vs, 852m, 830brs, 798sh, 752w, 723w, 670s, 637vw, 615w, 545vw, 450br.w, 362vs, 270vw, 238s. Anal. Calcd. for $C_{23}H_{47}NSi_2Fe$: C, 61.43; H, 10.53; N, 3.12. Found: C, 61.17; H, 10.21; N, 2.95. The E.I. mass spectrum showed a molecular ion at $m/e$ = 449 amu. The parent ion isotopic cluster was simulated: (calcd. %, observd. %): 447(6, 6), 448(2, 3), 449(100, 100), 450(38, 39), 451(14, 13), 452(3, 2).

*[Cp′FeN(SiMe$_3$)(CMe$_3$)] (**2b**).* A mixture of **1** (1.41 g, 1.7 mmol) and $[Li\{N(SiMe_3)(CMe_3)\}(OEt_2)]_2$ (0.76 g, 1.7 mmol) was dissolved in about 20 mL of pentane, and the reaction mixture turned immediately bright yellow. The solution was stirred for 10 min and filtered. The solvent was removed under reduced pressure, and the yellow residue was crystallized from $O(SiMe_3)_2$ (ca. 5 mL) at −30 °C to yield bright yellow blocks. Complex **2b** was sublimed slowly in a sealed ampule at 60−70 °C. Yield: 0.92 g (2.12 mmol, 62%). Mp 112−114 °C (rev.). $^1$H NMR ($C_6D_6$, 292K): $\delta$ 96.0 (9H, $CMe_3$, $\nu_{1/2}$ = 1840 Hz), 50.0 (9H, $SiMe_3$, $\nu_{1/2}$ = 1100 Hz), −27.4 (18H, Cp′-$CMe_3$, $\nu_{1/2}$ = 810 Hz), −40.0 (9H, Cp′-$CMe_3$, $\nu_{1/2}$ = 630 Hz). IR (Nujol mull; CsI windows; cm$^{-1}$): 1365s, 1240s, 1200s, 1110w, 1038m, 1005s, 960m, 865vs, 830brs, 780s, 750m, 722w, 680m, 670m, 632w, 600vw, 545m, 530m, 490m, 450m, 430w, 380s, 350vw, 320br.w, 260m, 230vbr.w. Anal. Calcd. for $C_{24}H_{47}NSiFe$: C, 66.49; H, 10.93; N, 3.23. Found: C, 66.03; H, 11.03; N, 3.15.

*[Cp′Fe(O-$\kappa^1$-OC$_6$H$_2$tBu$_3$-2,4,6)] (**4-CMe$_3$**).* A mixture of **2a** (0.18 g, 0.4 mmol) and freshly sublimed $HOC_6H_2tBu_3$-2,4,6 (0.104 g, 0.4 mmol) was dissolved in *n*-hexane (ca. 15 mL) and stirred at room temperature 20 min to form an orange-red solution. The volume was reduced to about 3 mL, and slow cooling to −25 °C yielded red crystals of **4-CMe$_3$** (0.09 g, 0.16 mmol, 41%). Mp 165−170 °C. $^1$H NMR ($C_7D_8$, 290 K): $\delta$ 118.5 (2H, *m*-CH, $\nu_{1/2}$ = 360 Hz), 27.6 (9H, *p*-$CMe_3$, $\nu_{1/2}$ = 50 Hz), −13.8 (18H, *o*-$CMe_3$, $\nu_{1/2}$ ~ 1800 Hz), −30.7 (9H, Cp′-$CMe_3$, $\nu_{1/2}$ ~ 800 Hz), −33.3 (18H, Cp′-$CMe_3$, $\nu_{1/2}$ ~ 1060 Hz) (the two Cp-$CMe_3$ resonances overlap). IR (Nujol mull; CsI windows; cm$^{-1}$): 1430w, 1300vw, 1270br.s, 1245s, 1200m, 1170vw, 1160vw, 1127w, 1025vw, 1005vw, 895w, 880w, 858m, 830m, 780w, 760w, 680w, 650w, 580s, 490br.w, 475br.w. Anal. Calcd. for $C_{35}H_{58}OFe$: C, 76.34; H, 10.62. Found: C, 75.98; H, 10.42.

*NMR Experiments of **2a** with HOC$_6$H$_3$tBu$_2$-2,6 and HOC$_6$H$_2$tBu$_2$Me.* In a screw-cap NMR tube **2a** (22.0 mg, 0.05 mmol) and $HOC_6H_2tBu_2R$ (10.3 mg (R = H) or 11.0 mg (R = Me)) were dissolved in $C_7D_8$. A color change from yellow to orange-red was observed on mixing, and the $^1$H NMR spectra of **4-H** and **4-Me** were recorded.

**4-H**: $^1$H NMR ($C_7D_8$, 289 K): $\delta$ 116.6 (2H, *m*-CH, $\nu_{1/2}$ ~ 400 Hz), −8.3 (9H, *p*-H, $\nu_{1/2}$ = 115 Hz), −12.7 (18H, *o*-$CMe_3$, $\nu_{1/2}$ ~ 2130 Hz), −29.9 (9H, Cp′-$CMe_3$, $\nu_{1/2}$ ~ 980 Hz), −32.1 (18H, Cp′-$CMe_3$, $\nu_{1/2}$ ~ 1060 Hz) (the two Cp-$CMe_3$ resonances overlap).

**4-Me**: $^1$H NMR ($C_7D_8$, 301 K): $\delta$ 118.5 (2H, *m*-CH, $\nu_{1/2}$ = 440 Hz), 103.4 (3H, *p*-Me, $\nu_{1/2}$ = 230 Hz), −15.8 (18H, *o*-$CMe_3$, $\nu_{1/2}$ ~ 2240 Hz), −30.5 (9H, Cp′-$CMe_3$, $\nu_{1/2}$ ~ 920 Hz), −34.2 (18H, Cp′-$CMe_3$, $\nu_{1/2}$ ~ 1200 Hz) (the two Cp-$CMe_3$ resonances overlap).

*[Cp′Fe($\eta^5$-O=C$_6$H$_3$tBu$_2$-2,6)] (**5-H**).* A mixture of **2a** (0.18 g, 0.4 mmol) and freshly sublimed $HOC_6H_3tBu_2$-2,6 (0.082 g, 0.4 mmol) was dissolved in *n*-hexane (ca. 15 mL) and stirred at room temperature to form an orange-red solution of **4-H**. The reaction mixture was heated to 45 °C for 16 h, and during this time the color changed to deep purple. The reaction mixture was filtered, concentrated, and cooled to yield deep purple crystals of **5-H**. Yield: 0.15 g (0.3 mmol, 76%). $^1$H NMR ($C_6D_6$, RT): $\delta$ 5.46 (2 H, d, $^3J_{HH}$ = 5.8 Hz, *m*-CH), 5.29 (1H, t, $^3J_{HH}$ = 5.8 Hz, *p*-CH), 4.17 (2H, Cp′-CH), 1.65 (18H, s, *o*-$CMe_3$), 1.43 (9H, s, Cp′-$CMe_3$), 1.21 (18H, s, Cp′-$CMe_3$). $^{13}$C{$^1$H} NMR ($C_6D_6$, RT): $\delta$ 157.8 (C=O), 104.9 (Cp′-*C*(4)), 102.2 (*o*-*C*), 93.4 (Cp-*C*(1,2)), 84.4 (*m*-*C*H), 68.6 (Cp′-CH), 66.5 (*p*-CH), 35.8 (*o*-$CMe_3$), 33.5 (6C, $CH_3$), 32.6 (2C, $CMe_3$), 32.4 (3C, $CH_3$), 31.9 (1C, $CMe_3$), 31.3 ($CH_3$). IR (Nujol mull; KBr windows; cm$^{-1}$): 1552s, 1513m, 1486m, 1316w, 1251br.m, 1240br.m, 1197vw, 1170w, 1110m, 1090m, 1023m, 995w, 945w, 919vw, 870s, 853m, 824vw, 806vbr.m, 741m. Anal. Calcd. for $C_{31}H_{50}OFe$: C, 75.28; H, 10.19. Found: C, 74.95; H, 10.15.

*[Cp′Fe($\eta^5$-O=C$_6$H$_2$MetBu$_2$-2,6)] (**5-Me**).* A mixture of **2a** (0.18 g, 0.4 mmol) and freshly sublimed $HOC_6H_2MetBu_2$ (0.088 g, 0.4 mmol) was dissolved in *n*-hexane (ca. 15 mL) and stirred at room temperature to form an orange-red solution of **4-Me**. The reaction mixture was heated to 45 °C for 16 h, and during this time the color changed to deep purple. The reaction mixture was filtered, concentrated, and cooled to yield deep purple crystals of **5-Me**. Mp 140−144 °C. Yield: 0.16 g (0.31 mmol, 79%). $^1$H NMR ($C_7D_8$, RT): $\delta$ 5.33 (2 H, s, *m*-CH), 4.21 (2H, s, Cp′-CH), 2.18 (3H, s, *p*-$CH_3$), 1.61 (18H, s, *o*-$CMe_3$), 1.41 (9H, s, Cp′-$CMe_3$), 1.25 (18H, s, Cp′-$CMe_3$). $^{13}$C{$^1$H} NMR ($C_6D_6$, RT): $\delta$ 157.7 (*C*=O), 104.6 (Cp′-*C*(4)), 98.5 (*o*-C), 94.6 (Cp′-*C*(1,2)), 84.3 (*m*-CH), 82.6 (*p*-*C*Me), 68.4 (Cp′-CH), 35.8 (*o*-$CMe_3$), 33.6 (6C, $CH_3$), 32.8 (2C, $CMe_3$), 32.4 (1C, $CMe_3$), 32.2 (3C, $CH_3$), 31.5 ($CH_3$), 21.9 (*p*-$CH_3$). IR (Nujol mull; KBr windows; cm$^{-1}$): 1563s, 1536s, 1482m, 1312w, 1258sh, 1247s, 1237sh, 1215m, 1201w, 1158s, 1119m, 1107m, 1030br.m, 995w, 946w, 926w, 865m,


dx.doi.org/10.1021/ic301770f | Inorg. Chem. 2012, 51, 11860−11872

810sh, 799m, 774w, 741w. Anal. Calcd. for $C_{32}H_{52}OFe$: C, 75.57; H, 10.31. Found: C, 75.32; H, 10.22.

*[Cp′Fe(μ-OC$_6$H$_3$tBu$_2$-3,5]$_2$* (**6**). A mixture of **2a** (0.18 g, 0.4 mmol) and freshly sublimed $HOC_6H_3tBu_2$-3,5 (0.082 g, 0.4 mmol) was dissolved in *n*-hexane (ca. 15 mL) and stirred at room temperature 20 min to form a green solution. The volume was reduced to about 3 mL and slow cooling to −25 °C yielded dark green crystals of **6***$C_6H_{12}$ (0.13 g, 0.12 mmol, 61%). The crystals contained one molecule of hexane per dimer which was verified by $^1$H NMR and elemental analysis. Mp 218−221 °C, accompanied with some decomposition. $^1$H NMR ($C_7D_8$, 290K): $\delta$ 99.6 (2H, Cp-CH/*o*-H, $\nu_{1/2}$ = 1200 Hz), −3.4 (18H, Cp′-CMe$_3$, $\nu_{1/2}$ = 220 Hz), −9.4 (9H, Cp′-CMe$_3$, $\nu_{1/2}$ = 190 Hz), −19.1 (18H, *m*-CMe$_3$, $\nu_{1/2}$ = 27 Hz), −49.7 (1H, *p*-H, $\nu_{1/2}$ = 30 Hz), −105.0 (2H, *o*-H Cp-CH, $\nu_{1/2}$ ∼ 500 Hz) IR (Nujol mull; CsI windows; cm$^{-1}$): 1600m, 1582m, 1425m, 1320sh, 1300m, 1260w, 1242m, 1235sh, 1215m, 1205m, 1160w, 1120m, 1030w, 1050w, 965 vs, 900w, 880w, 870vs, 822sh, 820vs, 692w, 685m, 642m, 605s, 580vw, 550vw, 465br.s, 405br.s, 365vw, 350br.w. Anal. Calcd. for $C_{68}H_{114}Fe_2O_2$: C, 75.95; H, 10.69. Found: C, 75.59; H, 10.34. The E.I. mass spectrum showed a molecular ion at *m*/*e* = 988 amu. The parent ion isotopic cluster was simulated: (calcd. %, observd. %): 986(12, 11), 987(9, 9), 988(100, 100), 989(74, 72), 990(29, 28), 991(8, 7), 992 (2,1)

*[Cp′Fe(N-κ$^1$-NHC$_6$H$_2$tBu$_3$-2,4,6)]* (**7**). A mixture of **1** (0.38 g, 0.46 mmol) and $[Li(NHC_6H_2tBu_3\text{-}2,4,6)(OEt_2)]_2$ (0.32 g, 0.47 mmol) was dissolved in about 20 mL of pentane. The reaction mixture turned yellow-brown immediately, and a colorless precipitate was formed. After the mixture was stirred for 10 min, the solvent was removed under dynamic vacuum. The residue was extracted with $O(SiMe_3)_2$ (ca. 4 mL), filtered, and the filtrate was concentrated to about 3 mL and cooled to −25 °C. Two crops of dark orange-brown crystals were isolated. Yield: 0.28 g (0.51 mmol, 55%). Mp 124−134 °C (dec.). $^1$H NMR ($C_6D_6$, 290 K): $\delta$ 108.2 (2H, *m*-CH, $\nu_{1/2}$ = 420 Hz), 24.1 (9H, *p*-CMe$_3$, $\nu_{1/2}$ = 45 Hz), 15.1 (18H, *o*-CMe$_3$, $\nu_{1/2}$ ∼ 2500 Hz), −24.7 (9H, Cp-CMe$_3$, $\nu_{1/2}$ ∼ 740 Hz), −26.7 (18H, Cp-CMe$_3$, $\nu_{1/2}$ ∼ 960 Hz) (the two Cp-CMe$_3$ resonances overlap). IR (Nujol mull; CsI windows; cm$^{-1}$): 3380s (N−H), 1765br.vw., 1610br.vw., 1380br.s, 1365s, 1350sh, 1262m, 1245s, 1200m, 1165m, 1120w, 1035br.w, 1005w, 960w, 924br.w., 885sh, 880s, 840s, 825s, 820sh, 775m, 755m, 720br.w., 690vw, 678m, 640m, 600vw, 580s, 545br.w., 495br.w, 480br.w., 450w., 380br.w, 260vbr.vw. Anal. Calcd. for $C_{35}H_{59}NFe$: C, 76.47; H, 10.82. Found: C, 76.03; H, 10.92.

*[Cp′Fe(N,C-κ$^1$,η$^5$-C$_6$H$_5$NPh)Fe(N-κ$^1$-NPh$_2$)Cp′]* (**8**). A mixture of **2a** (0.18 g, 0.4 mmol) and freshly sublimed $Ph_2NH$ (0.068 g, 0.4 mmol) was dissolved in toluene (ca. 5 mL) and heated to 65 °C for 20 h (without stirring) to form a dark red solution from which small a amount of a red crystalline material had already precipitated. The solution was allowed to cool to ambient temperature, and the volume of the solution was reduced to about 3 mL. Slow cooling to −25 °C yielded additional dark red crystals of **8**. Total yield: 0.09 g (0.10 mmol, 49%). Mp 162−182 °C (dec.). IR (Nujol mull; KBr windows; cm$^{-1}$): 1583m, 1532s, 1482m, 1343m, 1282s, 1241w, 1204w, 1173w, 1150vw, 1077vw, 1023w, 996w, 950vw, 915vw, 871w, 818m, 753m, 698m, 671w, 560vs, 548vs, 520s, 490m. Anal. Calcd. for $C_{58}H_{78}N_2Fe_2$: C, 76.14; H, 8.59; N, 3.06. Found: C, 75.77; H, 8.34; N, 3.15.

*[Cp′FeCH(SiMe$_3$)$_2$]* (**9**). A mixture of **1** (0.7 g, 0.84 mmol) and $LiCH(SiMe_3)_2$ (0.33 g, 2.0 mmol) was dissolved in about 60 mL of pentane. The reaction mixture turned yellow-orange immediately. After the mixture was stirred for 2 h, the solution was filtered and the pentane was removed under reduced pressure. The yellow-orange residue was sublimed in diffusion pump vacuum at 60−65 °C to give golden, crystalline material (0.50 g, 1.1 mmol, 66%). Mp 110−112 °C (rev.). $^1$H NMR ($C_6D_6$, 290 K): $\delta$ 38.7 (18H, SiMe$_3$, $\nu_{1/2}$ = 810 Hz), −35.3 (27H, CMe$_3$, $\nu_{1/2}$ = 1030 Hz, two resonances overlapped). IR (Nujol mull; CsI windows; cm$^{-1}$): 2815w, 1610br.vw., 1370sh, 1362s, 1348sh, 1285w, 1255m, 1245vs, 1205m, 1165sh, 1150w, 1110vw, 1035sh, 1010s, 955w, 920vw, 830vbr.vs, 775sh, 770s, 732s, 722sh, 680vs, 665vs, 610vs, 545m, 488s, 445m, 410vw, 370m, 340w, 280sh, 268m, 230s. Anal. Calcd. for $C_{24}H_{48}Si_2Fe$: C, 64.25; H, 10.78. Found: C, 63.99; H, 10.84. The E.I. mass spectrum showed a molecular ion at *m*/*e* = 448 amu. The parent ion isotopic cluster was simulated: (calcd. %, observd. %): 446(6, 5), 447(2, 3), 448(100, 100), 449(39, 40), 450(14, 14), 451(3, 2).

*[Cp′Fe(CO)$_2$(C(O)CH(SiMe$_3$)$_2$)]* (**10**). [Cp′FeCH(SiMe$_3$)$_2$] (**9**) (0.12 g, 0.27 mmol) was dissolved in 10 mL of pentane. The headspace was evacuated and replaced with CO (1 atm). The solution was stirred at ambient temperature for 20 h, and the solvent was removed under dynamic vacuum. The yellow residue was dissolved in hexamethyldisiloxane (ca. 4 mL) and filtered. The yellow-orange solution was concentrated and cooled to −30 °C to give yellow blocks (85 mg, 0.16 mmol, 60%). $^1$H NMR ($C_6D_6$, RT): $\delta$ 4.56 (s, ring-C*H*, 2H), 3.22 (s, C*H*(SiMe$_3$)$_2$, 1H), 1.32 (s, CMe$_3$, 18H), 1.27 (s, CMe$_3$, 9H), 0.32 (s, SiMe$_3$, 18H). $^{13}$C{$^1$H} NMR ($C_6D_6$, 300 K): $\delta$ 250.4 (1C, *C*(O)CH(SiMe$_3$)$_2$), 219.2 (2 C, CO), 110.7 (2C, ring-*C*CMe$_3$), 110.4 (1C, ring-CCMe$_3$), 94.2 (2C, ring-CH), 66.7 (1C, *C*H(SiMe$_3$)$_2$), 33.7 (6C, *C*H$_3$), 32.8 (2C, *C*Me$_3$), 31.7 (6C, C*H*$_3$), 31.3 (1C, 6C, *C*H$_3$), 1.9 (3C, Si*Me*$_3$). Anal. Calcd. for $C_{23}H_{48}OSi_2Fe$: C, 61.03; H, 10.69. Found: C, 61.32; H, 10.76.

*[{Cp′Fe(CO)$_2$}$_2$]* (**11**). [Cp′FeCH(SiMe$_3$)$_2$] (**9**) (0.12 g, 0.27 mmol) was dissolved in 10 mL of pentane. The headspace was evacuated and replaced with a 7:3 mixture of $H_2$ and CO (1 atm). The solution changed color from yellow to red-violet and was stirred at ambient temperature for 20 h. The solvent was removed under dynamic vacuum. The dark red-violet residue was dissolved in pentane, filtered, concentrated, and cooled to −30 °C to give red-violet crystals (0.04 g, 0.06 mmol, 42%). IR (toluene; KBr windows; cm$^{-1}$): 1934 (s, CO), 1765 (s, CO). $^1$H NMR ($C_6D_6$, RT): $\delta$ 4.80 (s, ring-C*H*, 4H), 1.37 (s, CMe$_3$, 36H), 1.35 (s, CMe$_3$, 9H). Anal. Calcd. for $C_{38}H_{58}Fe_2O_4$: C, 66.13; H, 8.47. Found: C, 66.33; H, 8.56. Complex **11** was previously prepared by another synthetic route.[80]

*Kinetic Study for the Conversion of 4-H/Me to 5-H/Me.* In a screw-cap NMR tube, **2a** (22.0 mg, 0.05 mmol) and $HOC_6H_2tBu_2R$ (10.3 mg (R = H) or 11.0 mg (R = Me)) were dissolved in $C_6D_6$ (500 μL). As internal standard 1,3,5-$(F_3C)_3C_5H_3$ (5 μL) was added to the $C_6D_6$ solution. Complexes **4-H/Me** formed rapidly upon mixing as indicated by a color change from light yellow to orange-red. The NMR sample was inserted into a temperature-calibrated probe, and the rearrangement of **4-H/Me** to **5-H/Me** was monitored by $^1$H NMR spectroscopy over approximately 2 half-lives. The decay of the *m*-CH resonance for **4-H/Me** was converted to concentration and fitted to a first-order plot of ln [**4-H/Me**] vs time, which gave observed rate constants as the slope. Sample graphs of the kinetic data can be found in the Supporting Information, Figures S9 and S10.

**Computational Details.** All calculations employed the long-range dispersion-corrected Grimme's functional (B97D).[71] The calculations were carried out with Gaussian 09 and no symmetry restrictions imposed ($C_1$). C, H, O, N, and Fe were represented by an all-electron 6-311G(d,p) basis set. Unrestricted calculations were performed for all paramagnetic species studied. The nature of the extrema (minima and transition states) was established with analytical frequencies calculations. The zero point vibration energy (ZPE) and entropic contributions were estimated within the harmonic potential approximation. The Gibbs free energy, $\Delta G$, was calculated for $T$ = 298.15 K and 1 atm. Geometrical parameters were reported within an accuracy of $10^{-3}$ Å and $10^{-1}$ degrees.

## ■ ASSOCIATED CONTENT

### Ⓢ Supporting Information

Crystallographic information files (CIF), VT-NMR data, details of the DFT calculations and mol2-files of all calculated structures, and comparison of experimental and computational structural data. This material is available free of charge via the Internet at http://pubs.acs.org.

## ■ AUTHOR INFORMATION

### Corresponding Author

*E-mail: mwalter@tu-bs.de.

### Notes

The authors declare no competing financial interest.

## ■ ACKNOWLEDGMENTS

We thank the Alexander von Humboldt Foundation for a Feodor-Lynen Fellowship (M.D.W.) and Prof. Maurice Brookhart for providing financial support (through NSF Grant CHE-0615704) and laboratory facilities (M.D.W.) during the initial phase of this research program. M.D.W. gratefully acknowledges the current financial support by the Deutsche Forschungsgemeinschaft (DFG) through the Emmy-Noether program (WA 2513/2-1).

## ■ REFERENCES

(1) Holland, P. L. *Can. J. Chem.* **2005**, *83*, 296.
(2) Holland, P. L. *Dalton Trans.* **2010**, *39*, 5415.
(3) Hendrich, M. P.; Gunderson, W.; Behan, R. K.; Green, M. T.; Mehn, M. P.; Betley, T. A.; Lu, C. C.; Peters, J. C. *Proc. Nat. Acad. Sci.* **2006**, *103*, 17107.
(4) Peters, J. C.; Mehn, M. P. In *Activation of Small Molecules*; Tolman, W. B., Ed.; Wiley-VCH: Weinheim, Germany, 2006; p 81.
(5) (a) Holland, P. L. *Acc. Chem. Res.* **2008**, *41*, 905. (b) Smith, J. M.; Subedi, D. *Dalton Trans.* **2012**, *41*, 1423.
(6) Vogel, C.; Heinemann, F. W.; Sutter, J.; Anthon, C.; Meyer, K. *Angew. Chem., Int. Ed.* **2008**, *47*, 2681.
(7) Scepaniak, J. J.; Fulton, M. D.; Bontchev, R. P.; Duesler, E. N.; Kirk, M. L.; Smith, J. M. *J. Am. Chem. Soc.* **2008**, *130*, 10515.
(8) Scepaniak, J. J.; Young, J. A.; Bontchev, R. P.; Smith, J. M. *Angew. Chem., Int. Ed.* **2009**, *48*, 3158.
(9) Scepaniak, J. J.; Vogel, C. S.; Khusniyarov, M. M.; Heinemann, F. W.; Meyer, K.; Smith, J. M. *Science* **2011**, *331*, 1049.
(10) Scepaniak, J. J.; Harris, T. D.; Vogel, C. S.; Sutter, J.; Meyer, K.; Smith, J. M. *J. Am. Chem. Soc.* **2011**, *133*, 3824.
(11) Nieto, I.; Ding, F.; Bontchev, R. P.; Wang, H.; Smith, J. M. *J. Am. Chem. Soc.* **2008**, *130*, 2716.
(12) Jové, F. A.; Pariya, C.; Scoblete, M.; Yap, G. P. A.; Theopold, K. H. *Chem.—Eur. J.* **2011**, *17*, 1310.
(13) Rodriguez, M. M.; Bill, E.; Brennessel, W. W.; Holland, P. L. *Science* **2011**, *334*, 780.
(14) Figg, T. M.; Holland, P. L.; Cundari, T. R. *Inorg. Chem.* **2012**, *51*, 7546.
(15) Chiang, K. P.; Scarborough, C. C.; Horitani, M.; Lees, N. S.; Ding, K.; Dugan, T. R.; Brennessel, W. W.; Bill, E.; Hoffman, B. M.; Holland, P. L. *Angew. Chem., Int. Ed.* **2012**, *51*, 3658.
(16) Campion, B. K.; Heyn, R. H.; Tilley, T. D. *J. Chem. Soc., Chem. Commun.* **1988**, 278.
(17) Loren, S. D.; Campion, B. K.; Heyn, R. H.; Tilley, T. D.; Bursten, B. E.; Luth, K. W. *J. Am. Chem. Soc.* **1989**, *111*, 4712.
(18) Fagan, P. J.; Mahoney, W. S.; Calabrese, J. C.; Williams, I. D. *Organometallics* **1990**, *9*, 1843.
(19) Koelle, U. *Chem. Rev.* **1998**, *98*, 1313.
(20) Strauss, D. A.; Zhang, C.; Quimbita, G. E.; Grumbine, S. D.; Heyn, R. H.; Tilley, T. D.; Rheingold, A. L.; Geib, S. J. *J. Am. Chem. Soc.* **1990**, *112*, 2673.
(21) Arliguie, T.; Chaudret, B. *J. Chem. Soc., Chem. Commun.* **1986**, 985.
(22) Trost, B. M.; Toste, F. D.; Pinkerton, A. B. *Chem. Rev.* **2001**, *101*, 2067.
(23) Dutta, B.; Scopelliti, R.; Severin, K. *Organometallics* **2008**, *27*, 423.
(24) Johnson, T. D.; Folting, K.; Streib, W. E.; Martin, J. D.; Huffman, J. C.; Jackson, S. A.; Eisenstein, O.; Caulton, K. G. *Inorg. Chem.* **1995**, *34*, 488.
(25) Sitzmann, H.; Dezember, T.; Kaim, W.; Baumann, F.; Stalke, D.; Kärcher, J.; Dormann, E.; Winter, H.; Wachter, C.; Kelemen, M. *Angew. Chem., Int. Ed. Engl.* **1996**, *35*, 2872.
(26) Wallasch, M.; Wolmershäuser, G.; Sitzmann, H. *Angew. Chem.* **2005**, *117*, 2653.
(27) Wallasch, M. W.; Rudolphi, F.; Wolmershäuser, G.; Sitzmann, H. *Z. Naturforsch. B* **2009**, *64*, 11.
(28) Wallasch, M. W.; Vollmer, G.; Kafiyatullina, A.; Wolmershäuser, G.; Jones, P. G.; Mang, M.; Meyer, W.; Sitzmann, H. *Z. Naturforsch. B* **2009**, *64*, 18.
(29) Wallasch, M. W.; Weismann, D.; Riehn, C.; Ambrus, S.; Wolmershäuser, G.; Lagutschenkov, A.; Niedner-Schatteburg, G.; Sitzmann, H. *Organometallics* **2010**, *29*, 806.
(30) Weismann, D.; Sun, Y.; Lan, Y.; Wolmershäuser, G.; Powell, A. K.; Sitzmann, H. *Chem.—Eur. J.* **2011**, *17*, 4700.
(31) Siemeling, U.; Vorfeld, U.; Neumann, B.; Stammler, H.-G. *Organometallics* **1998**, *17*, 483.
(32) Ohki, Y.; Hatanaka, T.; Tatsumi, K. *J. Am. Chem. Soc.* **2008**, *130*, 17174.
(33) Ohki, Y.; Takikawa, Y.; Hatanaka, T.; Tatsumi, K. *Organometallics* **2006**, *25*, 3111.
(34) Glöckner, A.; Daniliuc, C. G.; Freytag, M.; Jones, P. G.; Tamm, M. *Chem. Commun.* **2012**, *48*, 6598.
(35) Bartlett, R. A.; Ellison, J. J.; Power, P. P.; Shoner, S. C. *Inorg. Chem.* **1991**, *30*, 2888.
(36) Bartlett, R. A.; Olmstead, M. M.; Power, P. P.; Shoner, S. C. *Organometallics* **1988**, *7*, 1801.
(37) Stewart, J. L.; Andersen, R. A. *New J. Chem.* **1995**, *19*, 587.
(38) Yang, J.; Fasulo, M.; Tilley, T. D. *New J. Chem.* **2010**, *34*, 2528.
(39) Panda, A.; Stender, M.; Wright, R. J.; Olmstead, M. M.; Klavins, P.; Power, P. P. *Inorg. Chem.* **2002**, *41*, 3909.
(40) Harder, S.; Brettar, J. *Angew. Chem., Int. Ed.* **2006**, *45*, 3474.
(41) Pryadun, R.; Holm, R. H. *Inorg. Chem.* **2008**, *47*, 3366.
(42) Hashimato, M.; Urban, S.; Hoshino, R.; Ohki, Y.; Tatsumi, K.; Glorius, F. *Organometallics* **2012**, *31*, 4474.
(43) Danopoulos, A. A.; Braunstein, P.; Stylianides, N.; Wesolek, M. *Organometallics* **2011**, *30*, 6514.
(44) Merrill, W. A.; Stich, T. A.; Brynda, M.; Yeagle, G. J.; Fettinger, J. C.; De Hont, R.; Reiff, W. M.; Schulz, C. E.; Britt, R. D.; Power, P. P. *J. Am. Chem. Soc.* **2009**, *131*, 12693.
(45) Walter, M. D.; White, P. S. *New J. Chem.* **2011**, *35*, 1842.
(46) Walter, M. D.; Grunenberg, J.; White, P. S. *Chem. Sci.* **2011**, *2*, 2120.
(47) Walter, M. D.; White, P. S. *Dalton Trans.* **2012**, *41*, 8506.
(48) Bordwell, F. G. *Acc. Chem. Res.* **1988**, *21*, 456.
(49) *NMR of Paramagnetic Molecules*; La Mar, G. N., Horrocks, W. D., Holm, R. H., Eds.; Academic Press: New York, 1973.
(50) Bücken, K.; Koelle, U.; Pasch, R.; Ganter, B. *Organometallics* **1996**, *15*, 3905.
(51) It was also attempted to use *p*-OMe and *p*-Br substituted 2,6-di(*tert*-butyl)phenols for this investigation. However, while the monomeric pogo-stick molecules **4-OMe** and **4-Br** were readily formed (see Supporting Information for VT-NMR data) the arrangement process from **4-Br/OMe** → **5-Br/OMe** was not clean upon heating of the sample and significant amounts of decomposition products were also obtained precluding a kinetic analysis.
(52) Maekawa, M.; Daniliuc, C. G.; Freytag, M.; Jones, P. G.; Walter, M. D. *Dalton Trans.* **2012**, *41*, 10317.
(53) Walter, M. D., unpublished results.
(54) Iluc, V. M.; Hillhouse, G. L. *J. Am. Chem. Soc.* **2010**, *132*, 15148.
(55) Cowley, R. E.; Bontchev, R. P.; Sorrell, J.; Sarracino, O.; Feng, Y.; Wang, H.; Smith, J. M. *J. Am. Chem. Soc.* **2007**, *129*, 2424.
(56) Eckert, N. A.; Smith, J. M.; Lachicotte, R. J.; Holland, P. L. *Inorg. Chem.* **2004**, *43*, 3306.
(57) Walter, M. D.; White, P. S., manuscript in preparation.
(58) Betley, T. A.; Peters, J. C. *J. Am. Chem. Soc.* **2004**, *126*, 6252.
(59) Olmstead, M. M.; Power, P. P.; Shoner, S. C. *Inorg. Chem.* **1991**, *30*, 2547.
(60) Laskowski, C. A.; Hillhouse, G. L. *J. Am. Chem. Soc.* **2008**, *130*, 13846.
(61) Daida, E. J.; Peters, J. C. *Inorg. Chem.* **2004**, *43*, 7474.
(62) Brown, S. D.; Peters, J. C. *J. Am. Chem. Soc.* **2004**, *126*, 4538.

(63) Smith, J. M.; Lachicotte, R. J.; Holland, P. L. *Organometallics* **2002**, *21*, 4808.
(64) Zi, G. F.; Jia, L.; Werkema, E. L.; Walter, M. D.; Gottfriedsen, J. P.; Andersen, R. A. *Organometallics* **2005**, *24*, 4251.
(65) Walter, M. D.; Bentz, D.; Weber, F.; Schmitt, O.; Wolmershäuser, G.; Sitzmann, H. *New J. Chem.* **2007**, *31*, 305.
(66) Schröder, D.; Shaik, S.; Schwarz, H. *Acc. Chem. Res.* **2000**, *33*, 139.
(67) Carreón-Macedo, J.-L.; Harvey, J. N. *J. Am. Chem. Soc.* **2004**, *126*, 5789.
(68) Schrock, R. R.; Shih, K. Y.; Dobbs, D. A.; Davis, W. M. *J. Am. Chem. Soc.* **1995**, *117*, 6609.
(69) Jeffrey, J.; Lappert, M. F.; Luong-Thi, N. T.; Webb, M.; Atwood, J. L.; Hunter, W. E. *J. Chem. Soc., Dalton Trans.* **1981**, 1593.
(70) Scherer, O. J.; Hilt, T.; Wolmershäuser, G. *Organometallics* **1998**, *17*, 4110.
(71) Grimme, S. *J. Comput. Chem.* **2006**, *27*, 1787.
(72) There is a methodological uncertainty on the order of a few kcal/mol associated with DFT methods and open-shell systems. The dispersion-corrected Grimme B97D functional tends, in some cases, to overestimate dispersion and noncovalent interactions. Therefore the more crowded (complex) oxocyclohexadienyl structure might be overly stabilized. To exclude this phenomenon we also computed the energies of **4-CMe$_3$** and **5-CMe$_3$** with BP86 and B3LYP which does not take dispersion effects into account (see Supporting Information for details). The values obtained with BP86 are in complete disagreement with the experiment, since the oxocyclohexadienyl **5-CMe$_3$** is predicted to be significantly more stable than **4-CMe$_3$** by about 10 kcal/mol. In contrast B3LYP is in agreement with the experimental observation, but **4-CMe$_3$** is definitely overstabilzed compared to **5-CMe$_3$** with about 35 kcal/mol. The energetics obtained with B97D and B3LYP were also compared for the following reactions:

**2a** + $H_2NC_6H_2tBu_3$-2,4,6 → **7** + $HN(SiMe_3)_2$;
$\Delta G^{B97D}(298\ K) = -4.5$ kcal/mol;
$\Delta G^{B3LYP}(298\ K) = -1.3$ kcal/mol

**2b** + $H_2NC_6H_2tBu_3$-2,4,6 → **7** + $HN(SiMe_3)(CMe_3)$;
$\Delta G^{B97D}(298\ K) = -5.9$ kcal/mol;
$\Delta G^{B3LYP}(298\ K) = -5.9$ kcal/mol

**2a** + $Li[N(SiMe_3)(CMe_3)]$ ⇌ **2b** + $Li[N(SiMe_3)_2]$;
$\Delta G^{calc,B97D}(338\ K) = -5.9$ kcal/mol;
$\Delta G^{calc,B3LYP}(338\ K) = -1.9$ kcal/mol;
$\Delta G^{exp}(338\ K) = -0.32$ kcal/mol

**7** + $Li[N(SiMe_3)_2]$ ⇌ **2a** + $Li[NHC_6H_2tBu_3$-2,4,6];
$\Delta G^{calc,B97D}(298\ K) = -0.5$ kcal/mol;
$\Delta G^{calc,B3LYP}(298\ K) = -0.5$ kcal/mol;
$\Delta G^{exp}(298\ K) = -2.1$ kcal/mol

Overall while the absolute values predicted by B3LYP and B97D differ, both DFT functionals predict the same trends and energetic preferences.
(73) Sandström, J. *Dynamic NMR Spectroscopy*; Academic Press: New York, 1982.
(74) (a) Pangborn, A. B.; Giardello, M. A.; Grubbs, R. H.; Rosen, R. K.; Timmers, F. J. *Organometallics* **1996**, *15*, 1518. (b) Alaimo, P. J.; Peters, D. W.; Arnold, J.; Bergman, R. G. *J. Chem. Educ.* **2001**, *78*, 64.
(75) Çetinkaya, B.; Hitchcock, P. B.; Lappert, M. F.; Misra, M. C.; Thorne, A. J. *J. Chem. Soc., Chem. Commun.* **1984**, 148.
(76) Davidson, P. J.; Harris, D. H.; Lappert, M. F. *J. Chem. Soc., Dalton Trans.* **1976**, 2268.
(77) La Pierre, H. S.; Arnold, J.; Toste, F. D. *Angew. Chem., Int. Ed.* **2011**, *50*, 3900.
(78) Sur, K. *J. Magn. Reson.* **1989**, *82*, 169.
(79) Evans, D. F. *J. Chem. Soc.* **1959**, 2003.
(80) Hilt, T., Ph.D. Dissertation, Universität Kaiserslautern, Kaiserslautern, Germany, 1999.